QUANTIFICATION OF MINERALS ASSOCIATED TO ENAMEL CARIES

PROCESS BY RAMAN SPECTROSCOPY

by

Siras Sungkapreecha

Submitted to the Graduate Faculty of the School of
Dentistry in partial fulfillment of the requirements
for the degree of Master of Science in Dentistry,
Indiana University School of Dentistry, 2020.

Thesis accepted by the faculty of the Department of Cariology, Operative Dentistry & Dental Public Health, Indiana University School of Dentistry, in partial fulfillment of the requirements for the degree of Master of Science in Dentistry.

_____
Frank Lippert

_____
Anderson Hara

_____
Masatoshi Ando
Chair of the Research
Committee

_____
Norman Cook
Program Director

_____
Date

ACKNOWLEDGMENTS

LIST OF ILLUSTRATIONS

INTRODUCTION

PREVALENCE OF DENTAL CARIES

Dental caries is one of the most prevalent chronic diseases worldwide. According to the National Health and Nutrition Examination Survey, dental caries continues to be the most prevalent chronic disease in both children and adults in the US.[1] In 2012 National Center for Health Statistics reported that although dental caries has been declining in permanent teeth for many children since the 1960s, the report showed that dental caries in primary teeth for preschool children increased from 24 percent to 28 percent between 1988 and 2004. Furthermore, approximately 91 percent of U.S. adults aged 20 years to 64 years had dental caries in permanent teeth.[2] The World Health Organization (WHO) also indicated that dental caries is still a significant oral health problem, affecting 60 percent to 90 percent of children and the vast majority of adults.[3] In addition, the US Surgeon General also reported that dental caries is still the most common chronic childhood disease of children.[4]

The study from Bagramian et al. indicated that there is a marked increase in the prevalence of dental caries based on available epidemiological data from many countries. This affects primary as well as permanent teeth, and coronal as well as root surfaces.[3] Poor oral health from dental caries can potentially affect growth and early childhood development and could also lead to other serious health problems. Dental caries also has become a significant oral health problem among the elderly for various reasons such as higher retention of teeth and medication-induced hyposalivation.[5]

CHEMICAL COMPOSITION OF HUMAN ENAMEL

Sound enamel is highly mineralized tissue with non-uniform the chemical composition from the surface to inner structure.[6] Dental enamel contains 95 wt% to 98 wt% bioinorganic matter in the crystalline form carbonated calcium of hydroxyapatite [HA: $Ca_{10}(PO_4)_6(OH)_2$].[7] Calcium, phosphate, and fluoride concentrations are higher at the surface while magnesium, carbonate, and chloride concentrations are higher in the internal surface. In addition, concentration differences could vary from each location within the tooth itself. Enamel contains phosphate and carbonate approximately 17.5 percent to 18.5 percent and 2 percent to 4 percent by weight, respectively.[8] Enamel surface contains a high concentration of fluoride, calcium, and phosphate, which are less susceptible to acid challenge. On the other hand, the carbonate content was reported to be very minimal at the surface of enamel.[9] Carbonate has been found as a substitute for OH^-, PO_3^- in type A and B hydroxyapatite respectively.[10] There are significant correlations between carbonate content and enamel crystallinity with mechanical properties. As carbonate content increased, there was decreased modulus and hardness in enamel crystallinity.[11]

Under normal circumstances of a tooth, there is a dynamic process between demineralization and remineralization as described below.

$$Ca_{10}(PO_4)_6(OH)_2 + 8\ H^+ \leftrightarrow 10\ Ca^{2+} + 6\ HPO_4^{2-} + 2\ H_2O$$
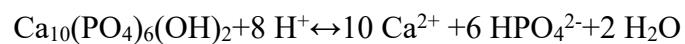
This chemical equilibrium proceeds from left to right vice versa depending on the chemical condition within the mouth. If demineralization overcomes remineralization, the acid produced by bacteria will contribute to dental caries.[12] When enamel, which contains 86-percent mineral by volume, is exposed to organic acids from a by-product of

acidogenic bacteria, the mechanical strength of enamel can be significantly reduced from demineralization, which can result in dental caries.[13] Calcified mineral including calcium, carbonate, and phosphate are loss from the tooth structure during demineralization.[14] The longer demineralization time, the deeper lesion depth, and higher mineral loss were found.[15] There is a correlation between carbonate content and mechanical properties of apatite crystals as when the carbonate content increases, the hardness of enamel decreases.[11]

ACTIVITY OF DENTAL CARIES

Demineralization of the tooth initiates when the rate of dissolution of mineral from tooth structure overcomes the rate of remineralization for long periods of time.[16] Although the signs of demineralization cannot be detected clinically at the very beginning, the dental caries is already initiated at a subclinical stage within the bacterial biofilm that covers tooth surfaces.[17] The early dental caries is non-cavitated and limited to the outer enamel surface. Early enamel caries can extend from 100 μm to 250 μm, to entirely through the enamel, and form cavitated lesions, which later progress into the underlying dentin.[18] In addition to caries severity assessment, caries activity assessment is also considered important information. Caries activity informed the probability of caries lesions to progress or arrest, by examining of the caries lesions and its surroundings. A continuous progression of demineralization is called active caries, and when progression is stopped, it is considered inactive/arrested caries. The determination of caries lesion activity is an important process in the treatment of dental caries because active lesions can be arrested by preventive management without surgical intervention.

There is no single predictor that accurately predicts caries activity.[19] Based on clinical examination, the presence of plaque, dull visual appearance, and rough tactile feeling indicate that lesions are active.[20] On the contrary, the lesions are considered inactive, if there is no plaque stagnation, luster visual appearance, and smooth tactile feeling. In addition, the gingival condition is also another predictor for the lesions close to the gingival line.[21]

Demineralization can be reversed to remineralization at any stages of dental caries through the uptake of calcium, phosphate, and fluoride from saliva. Thus, the determination of caries lesion activity is an essential process in the treatment of dental caries. Visual and tactile examinations are considered as a subjective assessment that provides information on the severity of the disease. Conversely, these examinations fall short in the assessment of the activity of the disease.[22] Currently, visual and tactile examinations are a conventional method for assessing the activity of dental caries.[23] However, differentiating between active and inactive lesions with visual and tactile examinations is still a problem to some of the dental practitioners, as they can demonstrate inconsistency in the clinical interpretation of the lesions.

VISUAL AND TACTILE EXAMINATIONS

When caries lesions are detected at an early stage, preventive treatment can be done to emphasize protective factors by preventive therapy, such as fluoride treatment, oral hygiene instructions, and dietary changes. Thus, nonsurgical preventive treatment has been recognized as preferable management of dental caries than irreversible invasive surgical treatment.[24] Furthermore, preventive treatment will result in long-term health and

economic benefits when compared to traditional restorative treatment.[25] Traditional and most common caries detection methods perform by most of the dental practitioners are visual and tactile examinations. Unfortunately, these methods have been demonstrated to have low sensitivity in detecting early caries lesions.[26] A comprehensive review showed caries detection sensitivity of 39 percent to 59 percent by visual examination in both the enamel and dentine of occlusal surfaces.[22] Moreover, the sensitivity of visual and tactile clinical examinations is mainly dependent on the examiner's experience and training. Although using a sharp explorer to detect dental caries could maximize the sensitivity of caries detection, it may cause an irreversible superficial cavity within the lesion.[27] In other words, the tooth structure of early caries lesions might be destroyed further by the use of explorer and accelerate the progress of caries lesions. In addition, differentiating between active and inactive caries with visual and tactile examinations is still a problem for dental practitioners.

BITEWING RADIOGRAPHY

Another conventional caries detection method is the radiographic examination. Bitewing radiography can be used to detect dental caries on approximal surfaces of posterior teeth. However, a systematic review showed that for approximal surfaces radiographs only had an overall sensitivity of 50 percent.[28] A radiograph can underestimate the actual extent of dental caries, once a lesion can be detected radiographically, caries has already penetrated into dentin, and restorative treatment may be needed.[29] These conventional examinations are suitable for the detection of advanced lesions but are not sufficient for the early caries lesions.

Current conventional clinical detection by visual and tactile examinations is not adequate to address the change in dental caries development. Moreover, these conventional examinations do not possess the sensitivity, specificity, or ability to account for the dynamic process of demineralization-remineralization nature. The development of refined early caries detection methods is needed in order to provide preventive treatment as early as possible. In addition, it would be beneficial that such method should assess caries activity of the lesion, which can define the progression or regression of existing dental caries in time.[30]

TECHNOLOGY-BASED CARIES DETECTION METHODS

In recent years, technology-based caries detection methods have been developed to identify the earliest mineral changes with improvements in sensitivity and specificity over traditional detection methods.[31]

Electrical Conductance

There has been a long history of using electrical conductance for the detection of dental caries as this concept was first introduced in 1956 by Mumford.[32] Electronic Caries Monitor (ECM) is the device that based on the difference of conductivity between a sound tooth and caries lesions; the more demineralized the tooth, the greater the electrical conductivity. Due to changes in porosity, saliva can penetrate into the pores of the demineralized enamel and increase the electrical conductivity of the tooth. Nevertheless, the specificity of this method is low, which increases the chance of false-positive and could lead to unnecessary irreversible operative treatment.[33]

Transillumination

Fiber-optic transillumination (FOTI) is a method that has been used since the 1970s.[34] FOTI uses a fiber probe with a white light that is placed on smooth surfaces of the tooth. Demineralized areas would appear darker compared to the sound tooth structure, and the contrast between sound and caries lesion can be detected. Although this technology showed high specificity, sensitivity is still relatively low. Moreover, this technology is subjective, with a high level of intra and inter-examiner variability.[35] Digital imaging fiber-optic transillumination (DIFOTI) has been introduced to overcome the reported large intra- and inter-examiner variability encountered.[14] In this method, the white light is delivered through an optical fiber via a specially designed handpiece that transfers the image back to a digital camera and visualizing the image on a monitor via a computer system. As with regular FOTI, the user's level of experience is essential. Some *in-vitro* studies indicated that DIFOTI has superior sensitivity for detection of approximal, occlusal, and smooth-surface caries when compared to radiographic findings.[36] Gutierrez et al. found that DIFOTI fails to detect early proximal caries and cannot be used for quantitative monitoring of early caries.[37] Most of the studies utilizing DIFOTI were conducted under laboratory conditions, and additional clinical studies are needed to examine the ability to detect caries lesions *in vivo*.[38] Near-infrared light transillumination (NILT) device such as DIAGNOcam (KaVo, Biberach, Germany) / CariVu (DEXIS, LLC, Hatfield, PA, USA) has been introduced recently. This device uses near-infrared light instead of visible light. One *in-vivo* study found that NILT shows equivalence to bitewing radiography for proximal caries detection.[39] However, additional clinical studies are needed in order to evaluate the diagnostics value of NILT.[40]

Fluorescence

Fluorescence is another method that can be used in caries detection. Using blue-green light (290- nm to 450-nm wavelength), Quantitative light-induced fluorescence (QLF, Inspektor Pro, The Netherlands) has been developed, and it measures the refractive differences between sound and demineralized enamel.[41] QLF is a nondestructive method that uses fluorescence spectroscopy to induce a natural fluorescence of the tooth as an indirect approach for measuring the mineral loss of tooth structure. The fluorescence images are filtered by a yellow high-pass filter (> 540 nm) and then captured by a color charge-coupled device camera. When compared with a sound tooth, the demineralized region appears as dark spots, and the fluorescent radiance of a caries lesion is lower than that of sound tooth structure. Fluorescence loss can be calculated by the difference between fluorescent radiance of sound enamel and caries lesion. QLF is a sensitive and reproducible technology for the quantification of enamel lesions on smooth surfaces.[42] Nonetheless, plaque, saliva, staining on the tooth surface, and the degree of dehydration may influence the validity of this method.[42]

Another method using red light (655 nm wavelength), such as DIAGNOdent (DD, KaVo, Biberach, Germany), has been developed for detection and quantification of dental caries on occlusal and approximal surfaces. Red light with 655-nm wavelength interacts with bacterial byproducts called porphyrins and then measured the reflected fluorescence. Both inorganic and organic molecules in the tooth absorb the light then the emitted fluorescence is collected and passed to the detector. The signal is processed and presented on display between 0 and 99. The value indicates proper treatment planning for each

lesion as observed, preventive treatment or restorative treatment. Even though some studies found that DD has excellent reproducibility,[43] this method could lead to false positives followed by unnecessary restorative treatments.[44]

Another recent technology-based caries detection method is Photothermal Radiometry-Modulated Luminescence (PTR/LUM, The Canary System, Toronto, Canada). PTR/LUM can detect the change of energy from the tooth and convert it into the light and thermal signals to detect the severity of dental caries.[45] One study compared the caries diagnostic ability of PTR/LUM, DD, visual and tactile examinations, and radiographs with the histological technique as the gold standard.[46] The authors found that PTR/LUM method is superior to all other methods in both sensitivity and specificity in enamel and dentin. However, there are a few published studies that have used this system in caries detection, and further studies are needed.[47]

Although these technology-based caries detection methods mentioned above hold significant promise, there is no clear evidence for any technology to be recommended as a substitute for visual and tactile examination.[48] The capability to quantify the degree of caries severity remains the main problem for these technology-based methods, together with intra and inter-examiner variability.[49] As a result, methods with improved sensitivity and specificity are needed for the detection of early caries lesions regarding both severity and activity.

Raman Spectroscopy

Optical spectroscopy, including fluorescence, reflectance, and Raman scattering, can provide information on hard tissue composition at the molecular level.[28] The Raman

effects were discovered by Chandrasekhara Venkata Raman in 1928. However, it was not utilized as an analytical tool until the introduction of the laser.[50] Raman spectroscopy can provide the most comprehensive data on the chemical composition; thus, it is a useful technique for studying the molecular structure. Highly specific information about proteins, lipids, carbohydrates, mineral orientation, and composition can be obtained by this technique.[51] A core process of Raman effects is the exchange between light and matter. When the light has an effect on an object, it can be scattered or absorbed. Most of the incident light and scattered light will have an identical frequency. The Raman effect is known as the process of energy exchange between scattering molecules of the object and incident light. Raman effect can be described as the transition of a molecule from its fundamental condition to an excited state with vibration, together with the absorption of an incident photon and emission of a Raman scattered photon of a molecule. The Raman scattered light can be displayed as a spectrum, exhibited as a function of molecular frequency change as each molecule has its pattern of vibration. A series of a band from each vibrational frequency of molecular properties can be considered as a fingerprint of a substance. Due to its property, Raman spectroscopy can be used in three ways - in statistical, chemical, and morphological studies.[30]

Spontaneous Raman spectroscopy (SpRS) or micro- Raman spectroscopy is the first type of Raman spectroscopy that has been developed. This technique based on Raman scattering by using visible normal far-field optics excitation. Nonetheless, when visible excitation is used, molecules show strong fluorescence that can interfere with the Raman spectrum.[30] The near-infrared Fourier transform (FT) Raman spectroscopy and polarized Raman spectroscopy were introduced later to offer a solution to fluorescence

problems. Recently, the stimulated Raman scattering spectroscopy (SRS) technique has been developed for tissue and cell imaging. SRS can enhance the Raman signal by 10^6 times when compared to visible excitation Raman spectroscopy. In the past, Raman spectroscopy was not considered as a practical option for biomedical applications due to its slower speed and the need for powerful stimulation sources. Recently, it is becoming significant in biomedical research for its excellent biochemical specificity and low water sensitivity. Raman spectroscopy has been used to diagnose pathologies of the oral cavity, gastrointestinal tract, brain tissue, and ocular tissue.[50]

Raman spectroscopy is suitable for the examination of mineralized tissues and has been used by various research groups to study bone and tooth structure.[52] This technique possesses several advantages such as non-destructive examination of samples with complex and uneven shapes without mechanical preparation, easy spectral analysis, and linear response to mineral concentrations. Raman spectroscopy can be used as a caries detection method from a biochemical characterization of hydroxyapatite based on peaks of phosphate vibrations from hydroxyapatite. In addition, Raman spectroscopy can inform biochemical signatures of early caries lesions because of a higher peak of phosphate intensity arising from hydroxyapatite when compared to a sound structure. The enamel rod arrangement of dental caries is changed when compared to normal enamel rod orientation from sound tooth structure, which results in the variation of Raman spectra.[31]

The aims of this study were:

1) To evaluate the ability of spontaneous Raman spectroscopy and stimulated Raman scattering spectroscopy to quantify phosphate and carbonate ratio (P/C-Ratio) in sound, demineralized and remineralized enamel, at different depths from the surface; and

2) To determine the correlation between outcomes of transverse microradiography (TMR: Integrated mineral loss [ΔZ] and lesion depth) and P/C-Ratio.

Hypothesis

Null hypothesis: spontaneous Raman spectroscopy and stimulated Raman scattering spectroscopy will not quantify demineralization and remineralization of enamel similar to transverse microradiography.

Alternative hypothesis: Spontaneous Raman spectroscopy and stimulated Raman scattering spectroscopy will quantify demineralization and remineralization of enamel similar to transverse microradiography.

REVIEW OF LITERATURE

RAMAN SPECTROSCOPY IN DENTAL
RESEARCH FOR SOUND TOOTH STRUCTURE

The first use of Raman spectroscopy in dental research was published in 1971. Rippon et al.[53] used visible excitation Raman spectroscopy for cellular analysis of mineralized and collagenous tissues in dentine. Later, a detailed orientation of single hydroxyapatite crystal in dental enamel has been carried out by Tsuda and Arends in 1994.[54] Micro-Raman spectroscopy (Spontaneous Raman spectroscopy or SpRS) was used in this study to examine a single crystal of synthetic hydroxyapatite and human enamel. Raman bands include the $PO_4{}^{3-}/OH^-$ with the spectral range from 180 cm^{-1} to 3600 cm^{-1} was observed. The authors found that intensities of the Raman bands are unchangeable to the orientation of the a- or b-axis but depend only on the c-axis orientation of a single crystal. The strongest bands are those of the $PO_4{}^{3-}$ vibrational mode at 959 cm^{-1}, which contains comparatively well-defined bands. This preliminary Raman study found strong orientation dependencies of phosphate/hydroxide similar to those of a single hydroxyapatite crystal have been observed among the bands in enamel spectra.

Another study from Tsuda et al. found that SpRS and near-infrared Fourier transform Raman spectroscopy (FRS) obtain vibrational spectra of minerals by analyzing scattered light from laser excitation. These methods have several advantages, including no sample preparation, easy analysis, and linear-response to mineral concentrations.[55] Authors also indicated that calcium fluoride is incorporated into human enamel by the

use of argon laser based SpRS. In addition, FRS can be used to obtain Raman signals for

identification of mineral components present in dental calculus. Sowa et al. reported

changes in carbonate concentration and apatite crystallinity in dental enamels with depth

by Fourier-transform Raman spectroscopy.[56] Intact human teeth were used without any

destructive preparation. The compositional and structural information was measured

from the enamel surface to 200-μm depth. The results showed that subsurface

carbonate gradient in the enamel could be observed from 10 μm to 100 μm and the

carbonate-to-phosphate ratio increases in deeper profile. In addition to carbonate

finding, depth profile clearly indicated, an increase in the phosphate content relative to

the protein content with increased depth.

Early Raman spectroscopy studies on human teeth have focused primarily on the

mineral composition of sound tooth structure. Later on, Raman spectroscopy was also

being used for caries research.

RAMAN SPECTROSCOPY IN CARIES RESEARCH

Hill and Petrou used FRS to characterize advanced natural dental caries lesions on

a human tooth without specimens preparation.[57] Raman spectra of enamel showed

characteristic bands of hydroxyapatite and collagen without luminescence. On the other

hand, spectra of caries tooth substance exhibited broadband luminescence with an

intensity similar to that of Raman scattering. The authors assumed that this luminescence

is due to microbiological products from bacteria in dental caries. The study also found

that the Raman spectra of tooth-colored resin composite restorations are different from

those of natural tooth substances. Therefore, Raman spectra can be used for the detection of such restorations.

Another study of dental caries by Raman Spectroscopy was done by Alex et al.[58] This study used SpRS for detecting natural early dental caries on extracted human teeth without specimen preparation. Authors indicated that sound enamel exhibited strong Raman polarization anisotropy of phosphate, whereas early caries consistently showed a reduced Raman polarization anisotropy. For sound enamel, the Raman peak arising with is strongly polarized from the vibration of PO_4^{3-} at 961 cm^{-1}. On the other hand, the spectra of carious lesions have weaker polarization dependence at 961 cm^{-1}. The observed differences in anisotropy are due to the alteration of hydroxyapatite crystal orientation in early caries enamel. The difference in the degree of Raman polarization anisotropy allows for differentiation between sound enamel and early dental caries.

According to a study by Mohanty et al., the intensity of the phosphate peaks of Raman spectra was found to differ significantly between sound enamel and demineralized enamel specimens.[59] This *in-vitro* study focused on early dental caries using SpRS. The demineralized enamel was developed by lactic acid on extracted human molars. Then, lesions were cross-sectioned and examined using SpRS. The intensity of the phosphate peaks to the degree of demineralization was compared by a series of Raman spectra over the cross-section area of the lesions. The study found that the body of the lesion is highly demineralized. Changes in the intensity of the phosphate peak at 961 cm^{-1} offer the most promise for detecting lesions. The results indicate that SpRS has both the sensitivity and selectivity to detect early dental caries.

The first remineralized study with SpRS was done by Zhan et al.[60] The authors evaluated the demineralization and remineralization in human dentin. Citric acid was used to simulate the erosive challenge demineralization for 10, 20, and 40 minutes. Then all samples were submerged to remineralization solution for 5 days. The peak intensities of inorganic composition (phosphate) decreased with the increase of acid etch time, while the peak intensities of the organic composition (amide) increased. In addition, the peak intensities of inorganic composition (phosphate) increased after remineralization treatment. This study showed that SpRS could be used to monitor the demineralization and remineralization status of dentin. The spectral changes of Raman intensity are attributed to mineral loss from demineralization in enamel induced by caries. In addition, the direction of rod arrangement changes in dental caries also affects Raman intensity. Ko et al. studied extracted natural teeth with white spots early caries lesion by SpRS.[58] The authors found a change in the peak intensities of phosphate as a result of a change in crystal orientation from the demineralization process. The results also showed that SpRS have high sensitivity and specificity (97 percent and 100 percent) in detecting early dental caries. Using the excitation with the laser at 785 nm, the typical Raman scattering spectrum of human enamel is detected with major bands corresponding to the PO_4^{3-} and CO_3^{2-}. For phosphate and carbonate, bands of the Raman scattering spectrum are dominated near 959 cm^{-1} and 1100 cm^{-1} respectively.[61] Raman band near 959 cm^{-1}, is the most intense band, assigned to the symmetric phosphate stretching vibration of phosphate ions (PO_4^{3-}) present in HA crystals.[62] Information on the state of the enamel is provided by the ratio of the 959 cm^{-1} Raman band intensities recorded. Hewko et al. used SpRS to detect early caries, and the results indicate the similar change in the polarization of the

Raman peak at 959 cm^{-1}, which referred to phosphate with altered integrity of the hydroxyapatite crystals.[63]

A comparative study has been done between Raman Spectroscopy and other technology-based caries detection methods. Kozloff et al. reported a comparative study of optical coherence tomography (OCT), histological appearance, and SpRS.[64] The authors concluded that phosphate peaks observed by SpRS could detect early dental caries similar to histological sections and OCT imaging. Carvalho et al. compared the sensitivity of Laser fluorescence and SpRS in early caries detection. The results concluded that both laser fluorescence and Raman spectroscopy could serve as a valuable tool in detecting early dental caries.[65] In recent years, novel variations of Raman spectroscopy have been developed to enhance the sensitivity and improve the spatial resolution.

STIMULATED RAMAN SCATTERING SPECTROSCOPY (SRS)

SRS in General Studies

The stimulated Raman scattering (SRS) spectroscopy technique has recently emerged as a powerful tool for label-free chemical imaging of cells and tissues. SRS spectroscopy has many attractive features, such as high biochemical specificity, inherent three-dimensional sectioning capability at the submicron spatial resolution, and deep tissue penetration depth. SRS signal is several orders of magnitude higher than that of a spontaneous Raman spectroscopy, making it a more efficient method. Thus, the result of SRS is more probable with a higher signal. The intensity of SRS imaging is significantly better than spontaneous Raman spectroscopy, which is achieved by implementing high-

frequency phase-sensitive detection. In addition, SRS microscopy offers background-free results with readily interpretable chemical contrast.[66]

There are two additional variants of SRS: surface-enhanced SRS and resonance SRS. Surface-enhanced SRS is suitable for molecules adsorbed on rough surfaces such as metal surfaces or nanostructures. Resonance SRS corresponds to a spontaneous Raman spectroscopy which is performed by a laser with a frequency close to the electronic transition of the subject in the study. However, it requires the use of highly strong x-ray lasers that might induce fluorescence artifact.[67] SRS can be used in various applications from a wide variety of fields such as the study of molecular conformational structures, material composition analysis, and ultrafast SRS imaging microscopy. All applications utilize the ability of SRS to detect a vibrational spectrum of all subjects in each study.

SRS has been used in medical studies since 2008. Freudiger et al. used SRS with a variety of biomedical applications, including differentiating distributions of omega-3 fatty acids and saturated lipids in cells, imaging of skin and brain tissues based on intrinsic lipid contrast, and observing medication delivery through the epidermis.[66] Ji et al. used SRS to detect brain tumor cells by implanted human brain cancer cells into mice, allowed them to infiltrate and grow into tumors, and then removed slices for SRS imaging.[68] The results showed that SRS was able to differentiate the two major components of brain tissue (lipid) and tumors (proteins). Another study by Ozeki et al. used SRS to produce multi-color images of the vessel in rat liver, and *in-vivo* spectral imaging of mouse ear skin.[69] SRS showed different constituents, spectral images which can extract small differences in spectral features. Saar et al. conducted a study of drug delivery to skin with SRS.[70] The high-speed three-dimensional imaging capability of SRS

reveals features that cannot be done with other methods, providing both kinetic

information and mechanistic insight of the drug delivery process.

SRS in Dental Research

Wang et al. reported the development and implementation of a

hyperspectral stimulated Raman scattering (SRS) spectroscopy technique for label-

free biomolecular imaging of the sound tooth.[71]

The hyperspectral SRS imaging technique developed covers fingerprint regions

for a tooth (800–1800 cm^{-1}). SRS imaging speed is more than 10^6 faster than confocal

Raman imaging without fluorescence background interference. Significant differences of

hyperspectral SRS spectra among dentin and enamel are observed, revealing the

biochemical composition differences.

SRS imaging also showed different polarization related to the molecular

orientation of specific tooth locations.

This study demonstrated the potential of SRS in rapidly characterizing

biochemical structures and compositions of a tooth together with

biomolecular orientation.

The first enamel demineralized study with SRS was done by Wang et al. in

2016.[72] The authors reported the utility of the SRS imaging technique developed for the

detection and characterization of early dental caries in the tooth. They found that

hyperspectral SRS images of the tooth covering both the regions can be acquired within

15 minutes. Hyperspectral SRS imaging reviewed the biochemical distributions across

the carious enamel. In addition, the mineral content in the body of lesion decreases by 55

percent when compared to the sound enamel. For surface zone mineral content increased

by 100 percent, indicating the formation of a hyper-mineralized layer. Moreover, polarized SRS imaging shows that the depolarization ratios of hydroxyapatite crystals of phosphate (959 cm^{-1}) which can be used for the detection of early dental caries. This study demonstrated that the SRS imaging technique could be used for quantitatively determining tooth mineralization levels and discriminating early dental caries from sound enamel, proving its potential of early detection of dental caries without labeling.

Another caries quantification study by SRS was done by Ando et al.[73] This study used SRS to quantify enamel demineralization by the phosphate-carbonate ratio (P/C-Ratio) and water content on bovine enamel. Each specimen was divided into 0 (sound), 8, 16, and 24 hours demineralization. SRS images were captured from the surface to 100 μm SRS intensities of phosphate (959 cm^{-1}), carbonate (1070 cm^{-1}), and water (3250 cm^{-1}) were obtained. The results showed that P/C-Ratio was higher in the sound area when compared to the demineralized area. For water content, the sound area has the lowest water content when compared to all demineralized areas. These results demonstrated the potential of using SRS microscopy for *in-vitro* and *in-situ* chemical analysis of early dental caries.

Phosphate and Carbonate Ratio (P/C-ratio)

Phosphate and carbonate were selected in this current study to use as an indicator for caries quantification because these two compositions can be measured by Raman spectroscopy. The first study about P/C-Ratio was published in 1948 by Sobel and Hanok.[74] This study reported P/C-Ratio of enamel and dentin using the upper incisor of the rat. The results found that P/C-Ratio varied from 2.08 to 7.72 in enamel, and from

4.40 to 9.31 in dentin. Another study by Hanok found the same trend of P/C-Ratio for enamel and dentine using the molars of the rat. Xu et al. used SpRS to measure carbonate and phosphate -ratio of human molars enamel; started at the outer enamel surface with 100 μm intervals and ended in the inner enamel near the dentin-enamel junction.[11] This study is the first investigation using SpRS to evaluate enamel carbonate content. The authors found that the carbonate peak intensity ($1070\ cm^{-1}$) gradually increased from outer surface to inner enamel which indicates a decrease in the degree of crystallinity of hydroxyapatite from outer enamel to the dentin-enamel junction. Based on the C/P-Ratio-Ratio generated via Raman spectra from Xu's study, recalculate P/C-Ratio ranged from 33 to 12.5 from the outer surface to inner enamel. Calcified mineral including calcium, carbonate, and phosphate are loss from the tooth structure during demineralization.[14] The longer demineralization time, the deeper lesion depth, and higher mineral loss were found.[15] There is a correlation between carbonate content and mechanical properties of apatite crystals as when the carbonate content increases, the hardness of enamel decreases.[11] According to a study by Robinson, phosphate lost is 18.5 percent, and carbonate is 1.0 percent on the lesion body of enamel caries. Based on these data, the P/C-Ratio should decrease as the severity of the demineralization increases, due to higher loss of phosphate when compared to carbonate.[75] These previous studies could demonstrate the potential of using SRS for chemical analysis of dental caries.

Raman spectroscopy has the potential to be used as caries monitoring based on mineral compsosition,[36,37] as Raman spectroscopy has been used only in caries quantification research thus far. However, no study on the caries process has been reported that compared Raman signal between demineralized and remineralized

specimens based on SpRS or SRS. Both SpRS and SRS could provide information about the caries process at the earliest stage and compare mineral identification between demineralized and remineralized areas on the same specimen. Currently, there is no study on the caries process, among sound, demineralized and remineralized enamel, based on SpRS and SRS has been reported to compare Raman signal of phosphate and carbonate. Moreover, most of the previous studies have been done with cross-sectioned of the tooth surface, not from the top of the surface.

MATERIALS AND METHODS

The sequence of this study is shown in Figure 1.

SPECIMEN PREPARATION

A total of 30, 5×5-mm bovine enamel specimens were prepared (one specimen

per tooth) and were mounted in polishing disks. First, the dentin side was grounded to a

flat uniform thickness (2.4mm) using 500-grit silicon carbide sandpapers (Struers Inc.,

Cleveland, PA, USA) with the Struers Polishing Unit – RotoPol Unit (Struers Inc.,

Cleveland, PA, USA). Specimens were removed from the disks and were remounted with

enamel side up on the disks. Subsequently, the enamel side was serially grounded to

create flat and parallel surfaces using 500-, 1200-, 2400-, and 4000-grit silicon carbide

sandpapers with the Struers Polishing unit. Specimens were polished using a 1-μm

diamond polishing suspension on a polishing cloth until the enamel surface was highly

polished. Then, specimens were rinsed with deionized water for 3 minutes in an

ultrasonic bath. Specimens with at least 0.5-mm enamel thickness and no obvious cracks

or flaws were selected (Figure 2). Specimens were stored in a sealable container with

moist paper towels to maintain integrity.

SPECIMEN DEMINERALIZATION

The enamel surfaces were cleaned with ethanol to achieve a grease-free and dry

surface. Each enamel surface was divided into 3 areas (1.67×5 mm^2 each); sound (No

treatment), 24h-demineralization, and 48h-demineralization. First, the sound and the 24h-

demineralization area of the enamel surface were covered with acid-resistant tape prior to

demineralization (Figure 3A). Specimens were exposed to 12.4-mL carbopol

demineralization solution at 37°C (Figure 3B). After 24 hours of demineralization (24h-Demin), the acid-resistant tape at the 24h-demineralization area was removed (Figure 3C). Then, specimens were exposed to a demineralization solution for an additional 24 hours at 37°C (Figure 3D: 48h-Demin). The carbopol demineralization solution contains 0.1 mol/l lactic acid and 0.2-percent carbopol 907TM (B.F. Goodrich Co. Chemical Group, Ohio, USA), saturated with hydroxyapatite and adjusted to a pH of 5.0. After demineralization treatment, deionized water was used to clean specimens.

DEMINERALIZED ENAMEL TRANSVERSE MICRORADIOGRAPHY (TMR) ASSESSMENT

After demineralization treatment, all specimens were mounted to an acrylic rod with cyanoacrylate gel near the end of the rod. Then, the acrylic rod was secured properly in mandril for cutting. One section, approximately 80 μm to120 μm in thickness with a surface-thickness variance ≤ 10% end-to-end, was cut from the center of each specimen using a 'Series 1000 Deluxe' hard tissue microtome (Microchrome Technology Inc., San Jose, CA) (Figure 4). Each thin-section were put into individual, 2-ml polystyrene analyzer cups containing a cotton pellet saturated with DI water. One of the remaining specimens was kept as a demineralized specimen, and the one remaining was later remineralized with pH cycling model.

All sections were mounted and analyzed using digital transverse microradiography (TMR-D). Thin sections of all specimens were transferred from polystyrene analyzer cups to glass plate. The glass plate with sections was placed in the TMR-D system and X-rayed at 45 kV and 45 mA at a fixed distance for 12 s. An aluminum step wedge (Custom made by Elbert de Josselin de Jong, INSPEKTOR) was x-

rayed under identical conditions for calibration. Then, the digital images were captured

by VHR X-Ray, USB Camera DFK 42BUC03 with Tamron Lens, and USB Camera

DFK 42BUC03 with CCS Macro Lens SE-16SM1 Assembled to XYZ Stage & Mounting

Plates. Images were analyzed using the TMR software v.3.0.0.18 (Inspektor Research

Systems BV, Amsterdam, The Netherlands). Sound enamel was assumed to be 87% v/v

mineral. The depth of the lesion and integrated mineral loss of 24h-Demin and 48h-

Demin were measured using TMR software (TMR for Windows; version 2.0.27.2;

Inspektor Research System, Amsterdam, The Netherlands). The following variables were

recorded: integrated mineral loss (ΔZ, product of lesion depth and the mineral loss over

that depth), lesion depth and mineral content at a distance from 0 μm (surface) up to 100

μm into the dentin-enamel junction (DEJ) at 10-μm intervals.

SPECIMEN REMINERALIZATION BY PH CYCLING MODEL

  After TMR assessment, one of the remaining specimens per specimen was

submitted to pH cyclic remineralizing daily treatments consisting of four, one-minute

remineralized treatments and a four-hour acid challenge and one acid challenge between

the second and third treatment.[76] Each specimen was placed on a 1-inch cube acrylic

block with sticky wax. Except for the enamel surface, specimens were covered with acid

resistance nail varnish (Avon True Color, Avon, USA). For the treatment of

remineralization periods, a slurry of a fluoridated dentifrice (1,100 ppm: Crest cavity

protection regular toothpaste, Crest, USA) was used for 1 minute. After each treatment,

the specimens were rinsed with running deionized water to remove any remaining paste.

Then specimens were submerged in freshly prepared synthetic saliva (0.9 mM $CaCl_2$-2

H_2O, 3mM KH_2PO_4, 130 mM KCl, 20 mM HEPES, 0.68 mM sodium citrate, pH

adjusted to 7.1 with KOH) for 60 minutes. For the acid challenge, the carbopol

demineralization solution was used for 4 hours followed by a deionized water rinse for 5

seconds and 60 minutes of saliva treatment. Specimens were then soaked in synthetic

saliva overnight. The daily cyclic system was repeated for 15 consecutive weekdays.

Over the weekend, the specimens were stored in a moist environment in a specimen cup

(Figure 5). After remineralization treatment, specimens were removed from the acrylic

block, and the nail varnish was removed by acetone.

RAMAN SPECTRA OF DEMINERALIZED AND REMINERALIZED
ENAMEL BY SPONTANEOUS RAMAN SPECTROSCOPY (SPRS)

Spontaneous Raman spectroscopy (SpRS) was carried out by Invia Renishaw

microscope with two lasers emitting 514.5 nm (argon laser) and 785nm (diode-pumped

laser) wavelength. During the recording of each single Raman spectrum, the laser beam

was spontaneously focused through a Leica 50 × long working distance microscope

objective with a numerical aperture of 0.5. The Raman spectra were recorded in the

rectangular area on the surface of specimens (FIGURE 6). Each paired specimen

(demineralized and remineralized enamel) was analyzed in six areas: for demineralized

specimen: sound (Sound-Demin), 24h-demineralization (24h-Demin), and 48h-

demineralization (48h-Demin); and for remineralized specimen: sound (Sound-Remin),

24h-Demin and 15 days remineralization (24hD-Remin), and 48h-Demin and 15 days

remineralization (48hD-Remin). The size of the SpRS image acquisition was 1×1 mm^2.

The analyses of the spectra were done by using WiRE 3.4 (Renishaw) software. The 959 cm^{-1} (phosphate) and 1060 cm^{-1} (carbonate) Raman band were fitted to the convolution of Gaussian and Lorentzian functions with the use of WiRE 3.4 software.

RAMAN SPECTRA OF DEMINERALIZED ENAMEL AND REMINERALIZED BY STIMULATED RAMAN SCATTERING SPECTROSCOPY (SRS)

Hyperspectral SRS imaging system was built based on a previously reported by Ando et. al.[73] Excitation sources were created by an ultrafast laser system with dual output operating at 80 MHz (InSight DeepSee, Spectra-Physics). The pump beam was originated from the tunable output with a pulse duration of 120 fs was tuned to 942 nm. Stokes beam, the other output centered at 1040 nm with a pulse duration of 220 fs was used. Pump beam and Stokes beam were modulated by an acousto-optic modulator (AOM, 1205-C, Isomet) at 2.3 MHz. An optical delay line was utilized in the pump light path, and a motorized translation stage (T-LS28E, Zaber) was employed to scan the delay between the two beams, then the spectral coverage from ~850 to 1150 cm−1 was tested. The pump and Stokes beams were sent into a home-built laser-scanning microscope. A 50× water immersion objective lens (NA 1⁄4 1.0, XLUMPLFLN-W, Olympus) was utilized to focus the light onto the specimens. The back-scattered signal was recorded by the same objective, reflected by a polarizing beam splitter to a lens, and then focused on a Si-photodiode (S3994-01, Hamamatsu). The SRS signal was extracted with a digital lock-in amplifier (HF2LI, Zurich Instrument).

Measurements were taken at six areas as described previously in Raman spectra of demineralized and remineralized enamel by spontaneous Raman spectroscopy (SpRS);

Sound-Demin, 24h-Demin, 48h-Demin, Sound-Remin, 24hD-Remin, and 48hD-Remin (Figure 7). SRS images (spectral coverage from ~850 to 1150cm^{-1}) were obtained (size 0.48 × 0.48 mm^2) with 10μm increments up to 100μm from the surface to the DEJ. By using surface-information (0 μm), SRS-intensity from phosphate and carbonate were measured. The spectra profile with two Lorentzian functions were fitted to obtain the peak-heights of phosphate and carbonate groups. The 959 cm^{-1} (phosphate) and 1060 cm^{-1} (carbonate) Raman band were obtained.

REMINERALIZED ENAMEL TMR ASSESSMENT

After SpRS and SRS image acquisition, all remineralized specimens were embedded in acrylic resin (Sampl-Kwick®, Buehler Ltd., Ill., USA) to prevent breaking the surface. One section, approximately 80-120 μm in thickness with a surface-thickness variance ≤ 10% end-to-end, was cut from the center of each specimen. Then, the depth of the lesion, integrated mineral loss and mineral percent of the remineralized area for 24h-Demin (24hD-Remin) and 48h-Demin (48hD-Remin) were determined in the same manner as described previously (Figure 8).

STATISTICAL ANALYSES

For TMR, mineral percent change was determined as follows: remineralized mineral content - demineralized mineral content (10μm interval). For SpRS and SRS on the surface (0 μm distance from the surface), peak-ratio was calculated as the phosphate peak height by carbonate peak height (P/C-Ratio). For SRS, P/C-Ratio was also measured with 10-μm increments up to 100 μm from the surface to the dentin-enamel junction.

Mean and standard deviation were determined for each parameter. Because the data were not normally distributed, Wilcoxon signed-rank tests were used to compare TMR, spontaneous Raman spectroscopy (SpRS), and stimulated Raman scattering spectroscopy (SRS) measurements between demineralized and remineralized for each group and between groups for demineralized and remineralized. Spearman correlation coefficients were calculated to assess the associations of all specimens (included both demineralized-remineralized specimens), demineralized specimens, remineralized specimens among TMR, SpRS, and SRS. A 5-percent significance level was used for each test.

SAMPLE SIZE JUSTIFICATION

Based on the results of the pilot study, the coefficients of variation for SMH change from baseline, SRS water content at 0 µm and 20 µm, SRS phosphate-carbonate, TMR mineral loss, and lesion depth are estimated to be 0.15 µm, 0.2 µm, 0.3 µm, 0.1 µm, 0.5 µm, and 0.55 µm, respectively, and the within-specimen correlation is estimated to be 0.5. With a sample size of 30 specimens, the study will have 80-percent power to detect differences between times of 12 percent for SMH change, 16 percent and 25 percent for SRS water content at 0 µm and 20 µm, 8 percent for SRS P/C-Ratio, 42 percent for TMR mineral loss, and 47 percent for TMR lesion depth.

RESULTS

TRANSVERSE MICRORADIOGRAPHY (TMR) ASSESSMENT

As demineralization time increased, both lesion depth and integrated mineral loss (ΔZ) increased. After the remineralization, both of them decreased. Table I presents the mean and standard deviation of TMR lesion depth and ΔZ for each group. For lesion depth, the result showed that 48h-Demin has a larger value than 24h-Demin; 48hD-Remin has a larger value than 24hD-Remin, and 48h-Demin has a larger value than 48hD-Remin with statistical significance (p <0.001). No statistical significance differences were found between 24h-Demin and 24hD-Remin. For ΔZ, the result showed that 48h-Demin has a larger value than 24h-Demin; 48hD-Remin has a greater value than 24hD-Remin, 24h-Demin has a larger value than 24hD-Remin, and 48h-Demin has a greater value than 48hD-Remin with statistical significance (p<0.001).

SPONTANEOUS RAMAN SPECTROSCOPY (SPRS) ASSESSMENT

For all treatment groups, as demineralized time increased, P/C-Ratio decreased. After remineralization, P/C-Ratio increased. Table II presents the mean and standard deviation of P/C-Ratio of SpRS for each group. 24hD-Remin had significantly larger P/C-Ratio than 24h-Demin (p $\leq$0.001). 48hD-Remin had a statistical significance greater P/C-Ratio than 48h-Demin (p $\leq$ 0.001). Sound-Demin had a statistical significance larger P/C-Ratio than 24h-Demin and 48h-Demin (p $\leq$ 0.001). 24h-Demin had a significantly larger value than 48h-Demin (p = 0.048). No statistical significance differences were found between Sound-Remin and 24hD-Remin (p = 0.316) and between 24hD-Remin and 48hD-Remin (p = 0.269)

STIMULATED RAMAN SCATTERING
SPECTROSCOPY (SRS) ASSESSMENT

As demineralized time increased, P/C-Ratio was decreased for all treatment groups. Table III presents the mean and standard deviation of P/C-Ratio of SRS for each group of distance from the surface. For Sound-Demin, 24h-Demin, and 48h-Demin, SRS P/C-Ratio was increased as the distance from the surface increased. For remineralized groups (Sound-Remin, 24hD-Remin, and 48hD-Remin), SRS P/C-Ratio was also increased as the distance from the surface increased. For demineralized groups, P/C-Ratio was decreased as the demineralized treatment increased.

DEMINERALIZED AND REMINERALIZED ENAMEL
COMPARISON (TABLE IV)

Sound Group

At 0 μm, 10 μm, 20 μm, Sound-Demin had significantly larger value than Sound-Remin (0 μm, $p = 0.042$; 10 μm, $p = 0.035$; 20 μm, $p = 0.027$).

At 30 μm, 40 μm, 50 μm, 60 μm, 70 μm, 80 μm, 90 μm, 100 μm, there was no statistical significance difference between Sound-Demin and Sound-Remin (30 μm; $p = 0.099$, 40 μm; $p = 0.301$, 50 μm; $p = 0.421$, 60 μm; $p = 0.384$, 70 μm; $p = 0.923$, 80 μm; $p = 0.810$, 90 μm; $p = 0.479$, 100 μm; $p = 0.301$).

24-hour Demineralization Group

At 0 μm, 10 μm, 20 μm, 30 μm, 40 μm, 50 μm, 60 μm, and 70 μm, there was no statistical significance difference between 24h-Demin and 24hD-Remin (0 μm, $p = 0.898$; 10 μm, $p = 0.835$; 20 μm, $p = 0.898$; 30 μm, $p = 0.936$; 40 μm, $p = 0.130$; 50 μm, $p = 0.099$; 60 μm, $p = 0.074$; 70 μm, $p = 0.092$).

At 80 µm, 90 µm, 100 µm, values for 24hD-Remin were significantly larger than for 24h-Demin (80 µm, p = 0.046; 90 µm, p = 0.017; 100 µm, p = 0.010).

48-Hour Demineralization Group

At every depth, there was no statistical significance difference between 48h-Demin and 48h-Remin (0 µm, p = 0.748; 10 µm, p = 0.724; 20 µm, p = 0.499; 30 µm, p = 0.440; 40 µm, p = 0.665; 50 µm, p = 0.748; 60 µm, p = 0.736; 70 µm, p = 0.974; 80 µm, p = 0.440; 90 µm, p = 0.350; 100 µm, p = 0.384).

Inter-Group Comparison (Table V)

After demineralized treatment, at 0 µm, 10 µm, 20 µm, 80 µm, 90 µm, 100 µm, the values for Sound-Demin were significantly greater than 24h-Demin (0 µm, p = 0.020; 10 µm, p = 0.037; 20 µm, p = 0.035; 80 µm, p = 0.023; 90 µm, p = 0.003; 100 µm, p = 0.002) and 48h-Demin (0 µm, p = 0.032; 10 µm, p = 0.023; 20 µm, p = 0.006; 80 µm, p = 0.024; 90 µm, p = 0.008; 100 µm, p = 0.013). No statistical significance differences were found between 24h-Demin and 48h-Demin (0 µm, p = 0.117; 10 µm. p = 0.109; 20 µm, p = 0.113; 80 µm, p = 0.125; 90 µm, p = 0.0162; 100 µm, p = 0.449).

At 30 µm, 40 µm, 50 µm, 60 µm, 70 µm, Sound-Demin was significantly higher than 48h-Demin (30 µm, p = 0.013; 40 µm, p = 0.024; 50 µm, p = 0.021; 60 µm, p = 0.007; 70 µm, p = 0.030). No statistical significance differences were found between Sound-Demin and 24h-Demin (30 µm, p = 0.092; 40 µm, p = 0.113; 50 µm, p = 0.157; 60 µm, p = 0.052; 70 µm, p = 0.085), and between 24h-Demin and 48h-Demin (30 µm, p = 0.152; 40 µm, p = 0.237; 50 µm, p = 0.212; 60 µm, p = 0.206; 70 µm, p = 0.0224).

After Remineralized Treatment

At 0 µm, 10 µm, 20 µm, 30 µm, 90 µm, no statistical significance differences were found between Sound-Remin and 24hD-Remin (p = 0.316), Sound-Remin and 48hD-Remin (p = 0.215), and 24hD-Remin and 48hD-Remin (p = 0.269)

At 40 µm, 50 µm, 60 µm, 70 µm, 80 µm, the values for 24hD-Remin were significantly larger than for 48hD-Remin. No statistical significance differences were found between Sound-Remin and 24hD-Remin, and between Sound-Remin and 48hD-Remin.

At 100 µm, the value for Sound-Remin was significantly larger than for 48hD-Remin. No statistical significance differences were found between Sound-Remin and 24hD-Remin, and between 24hD-Remin and 48hD-Remin.

CORRELATION

Statistical significance was achieved for any correlations larger than 0.20 in absolute values for correlations.

Correlation between SpRS and SRS (Table VI)

Positive correlation was found in demineralized groups (p < 0.05). No correlation was found for all specimens and the remineralized group.

Correlation between TMR Variables and Raman Spectroscopies (Table VII)

For SpRS, negative correlations were found. For SRS, negative correlation was found for the demineralized group and lesion depth. No correlations were found in the rest of the groups.

Correlation between TMR Mineral Percent and
SRS P/C-Ratio at Each Distance from the Enamel
Surface (Table VIII)

Positive correlation was found for the demineralized group at distances of 10 μm,

20 μm, 30 μm, 40 μm, 50 μm, and 60 μm from the surface. No correlation was found for

the demineralized group at a 70-μm, 80-μm, 90-μm, and 100-μm distance from the

surface for remineralized groups and mineral change.

FIGURES AND TABLES

```
┌─────────────────────────────────────────────────────┐
│        30 bovine specimens size 5 × 5 mm²             │
└─────────────────────────────────────────────────────┘
                          ⬇
┌─────────────────────────────────────────────────────┐
│      Specimen Demineralization for 0h, 24h, and 48h   │
└─────────────────────────────────────────────────────┘
                          ⬇
┌─────────────────────────────────────────────────────┐
│   Specimens were sectioned for TMR (separate into 2   │
│                       pieces)                         │
└─────────────────────────────────────────────────────┘
```

Demineralized specimens	Specimen remineralization by pH cycling 15 d.
⬇	⬇
SpRS and SRS measurement	Remineralized specimens
⬇	⬇
TMR analysis	SpRS and SRS measurement
	⬇
	Specimens were sectioned for TMR
	⬇
	TMR analysis
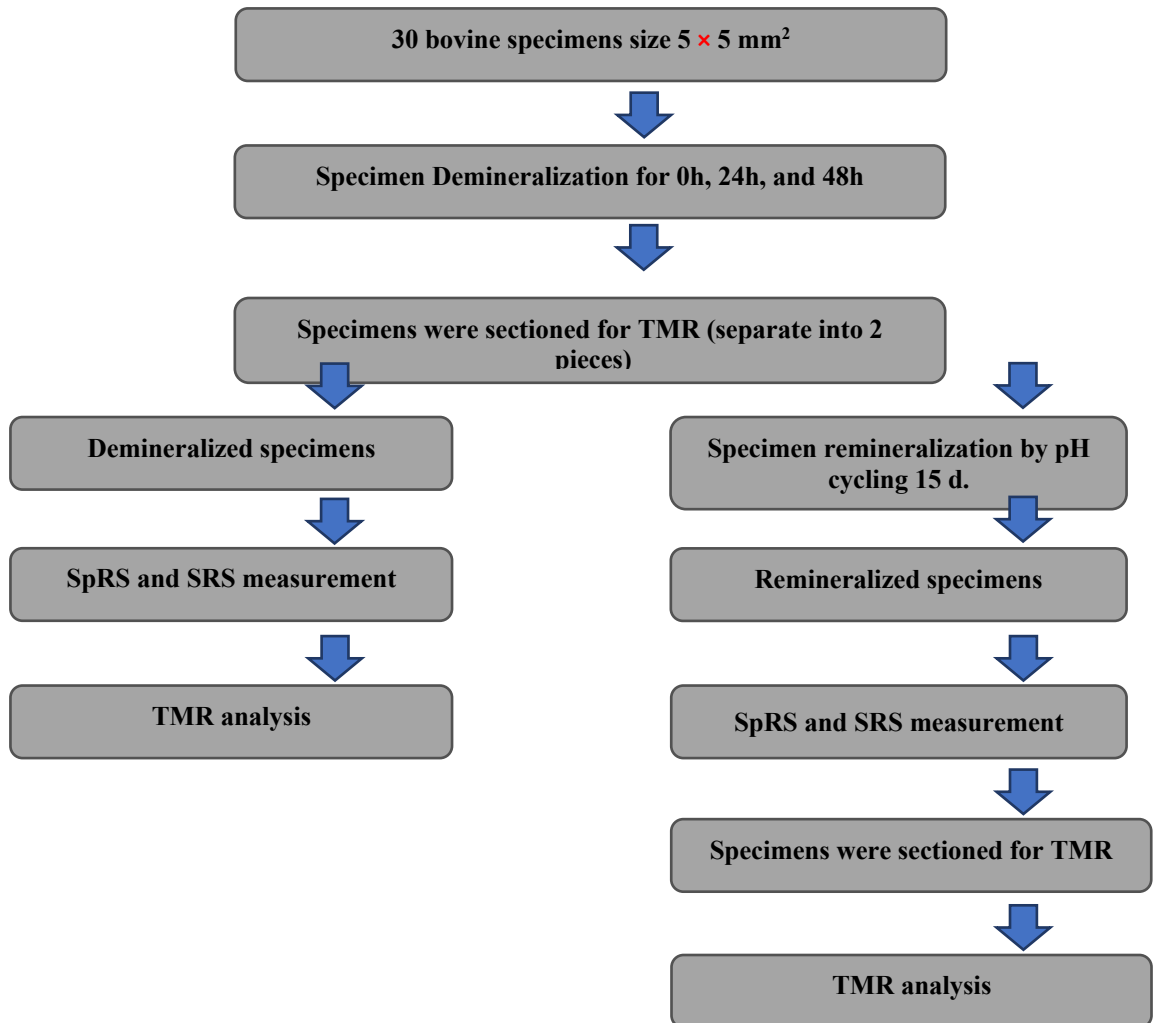
FIGURE 1. Flowchart of the study.
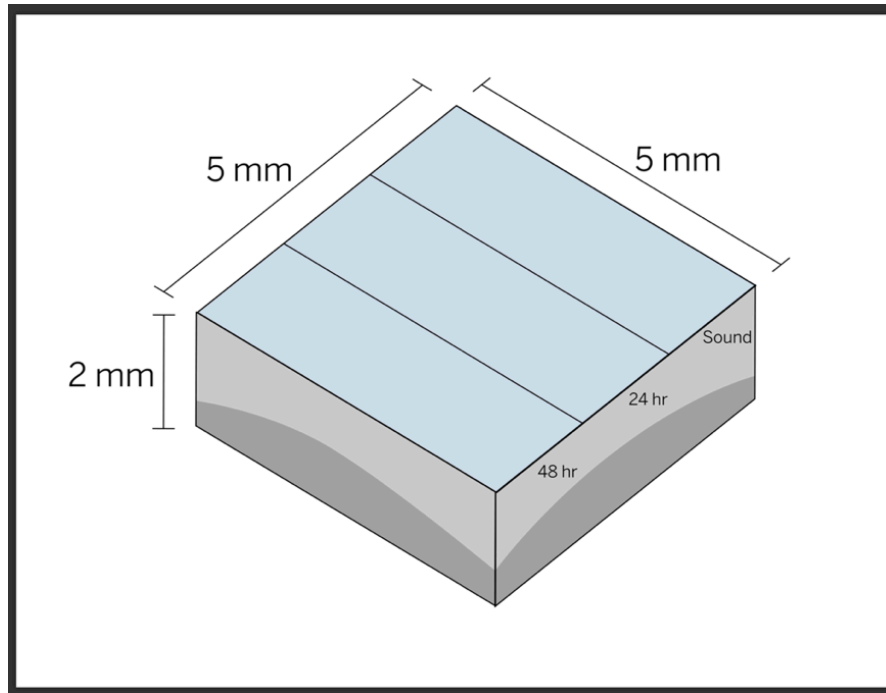
FIGURE 2.   An illustration shows dimensions of a bovine enamel specimen.
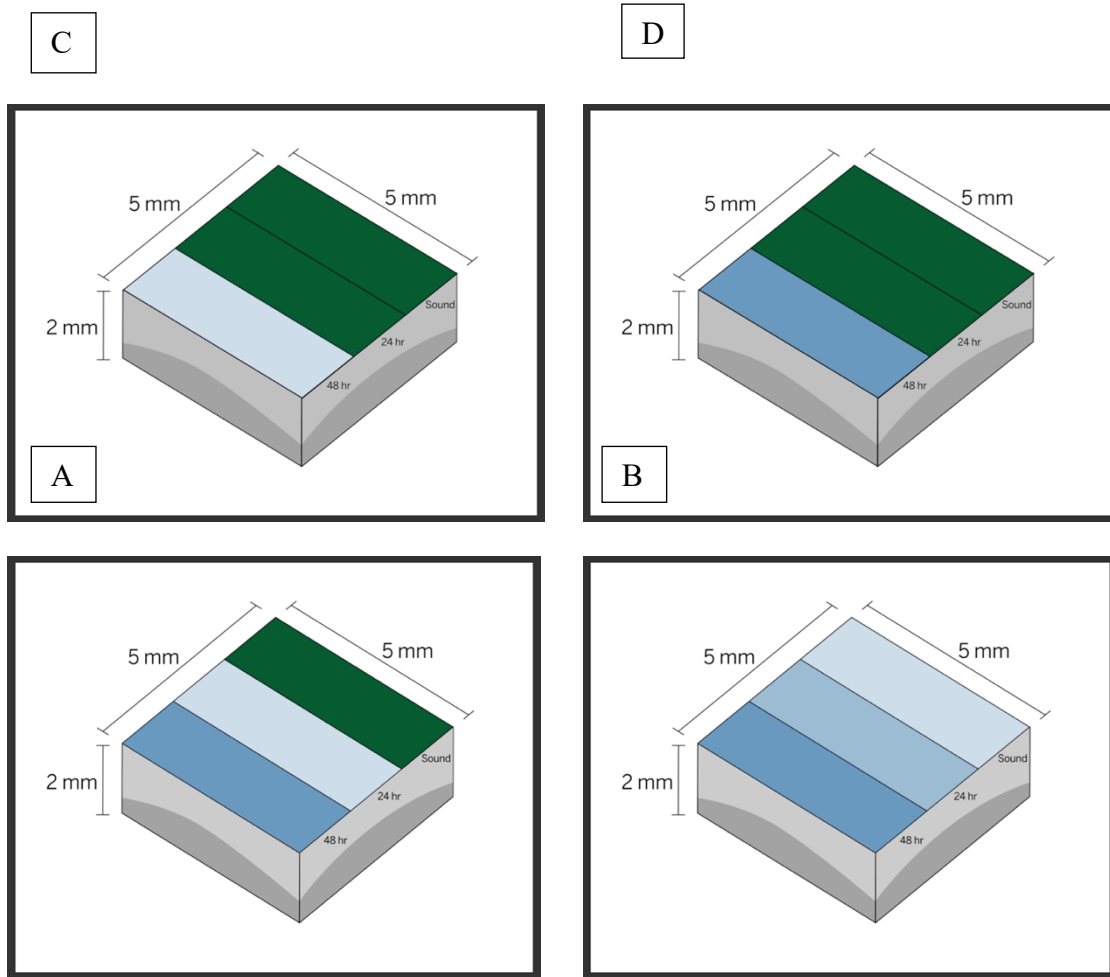
FIGURE 3.   An illustration shows a specimen demineralization process: (A) Sound and 24h-demineralization areas of enamel surface were covered with acid-resistant tape (green color) prior to demineralize. (B) Specimen after 24 hours demineralization. (C) After 24 hours demineralization, the acid-resistant tape at the 24h-demineralization area was removed. (D) Specimen after 48 hours demineralization.
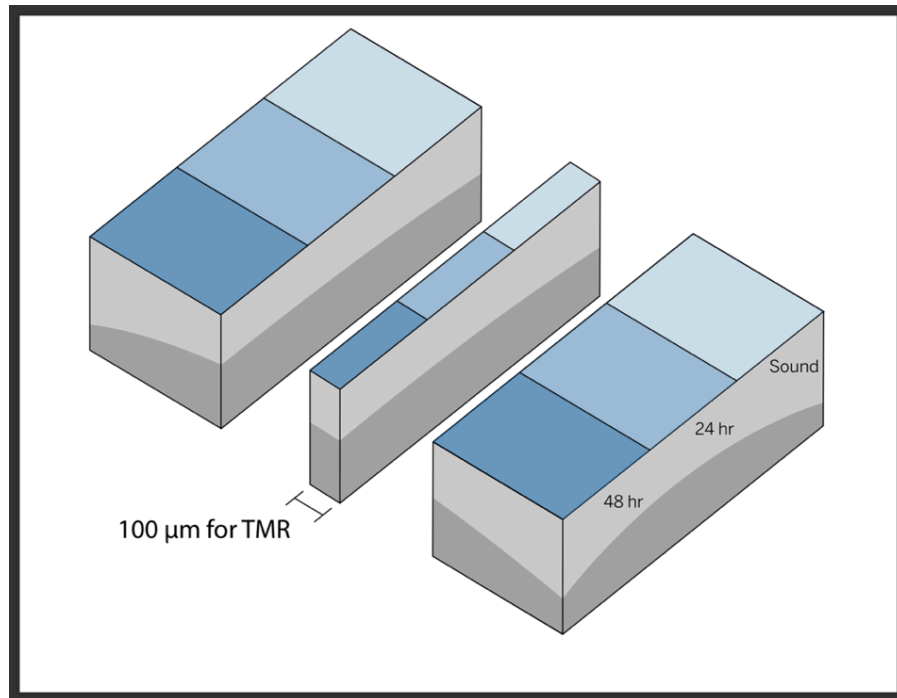
FIGURE 4.   An illustration shows one section, approximately 80-120 μm in thickness, was cut from the center of each specimen for TMR.
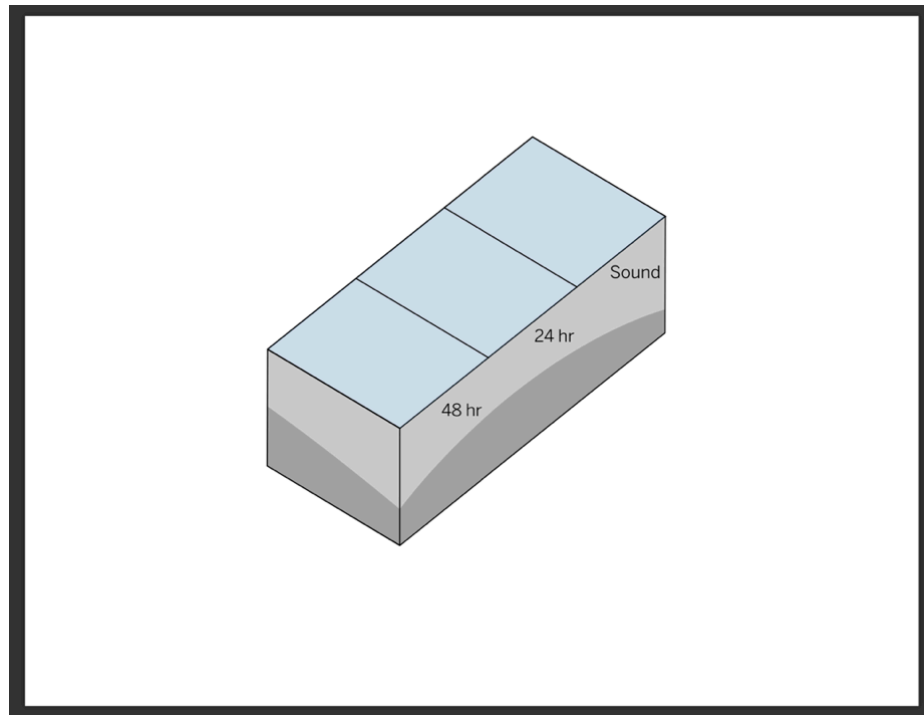
FIGURE 5.   An illustration shows a specimen after 15 days of remineralization treatment.
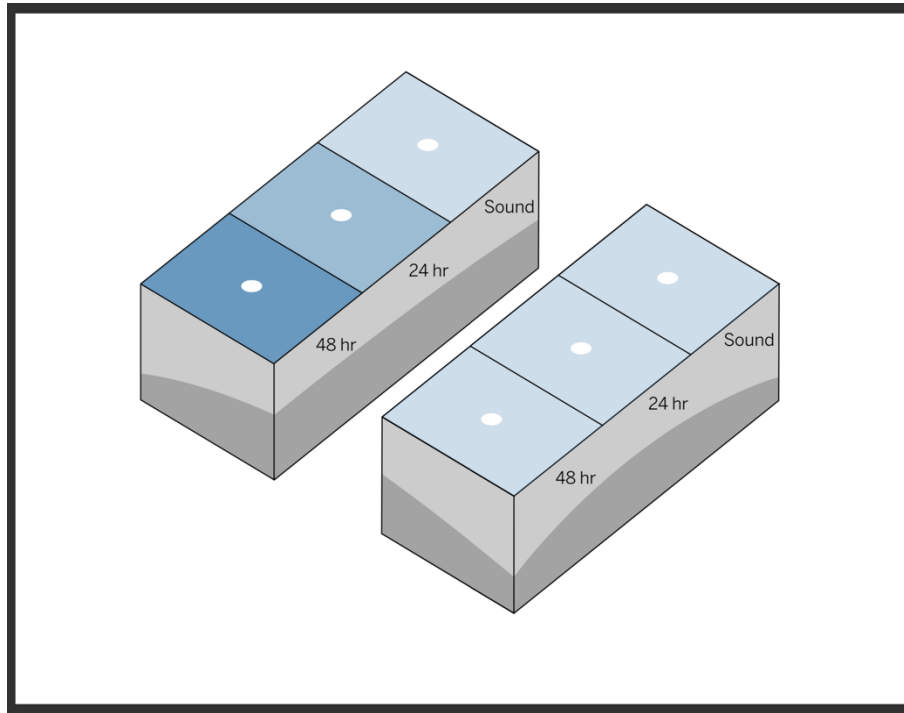
FIGURE 6.   An illustration shows the locations of analysis for Spontaneous Raman spectroscopy.
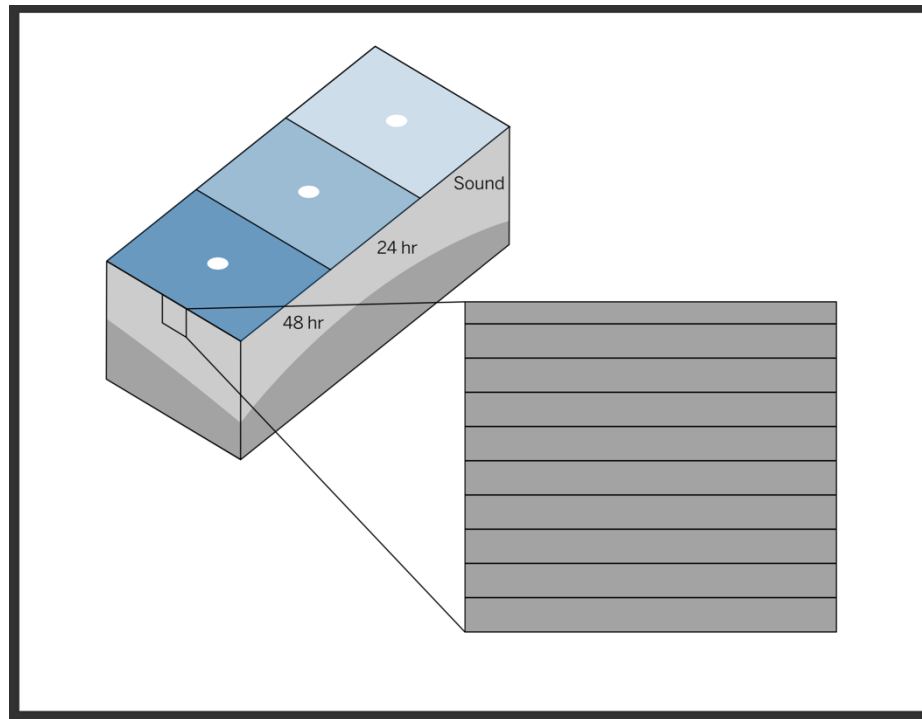
FIGURE 7.   An illustration shows specimens with an analysis by Stimulated Raman
Scattering spectroscopy
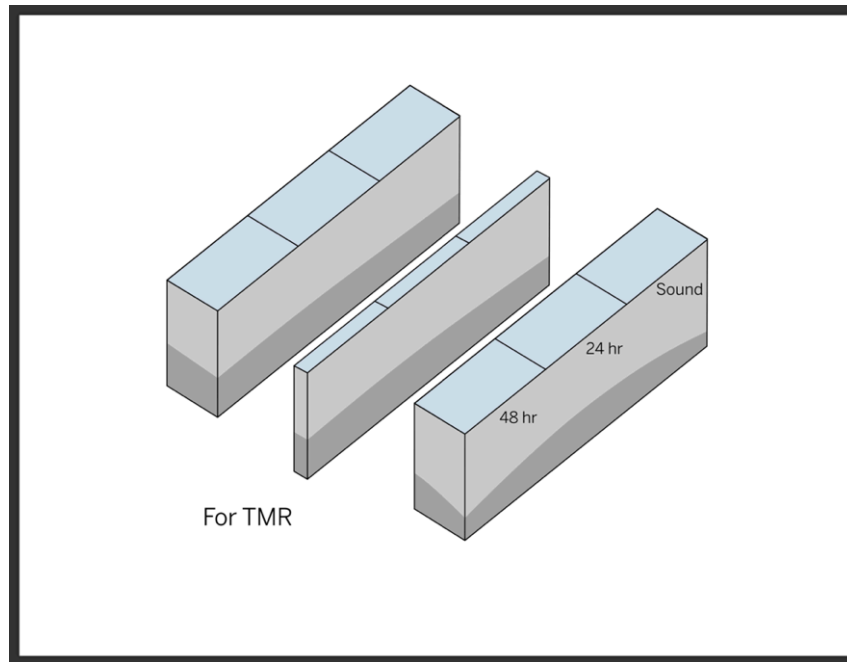
FIGURE 8. An illustration shows one section, approximately 80 μm to 120 μm in thickness, was cut from the center of each of remineralized specimen for TMR.

FIGURE 9.   A figure shows the sectioning of the specimen by Series 1000 Deluxe' hard tissue microtome.

FIGURE 10. A figure shows X-ray instrument (VHR X-Ray, USB Camera DFK
42BUC03 with Tamron Lens).

FIGURE 11.   A figure shows Spontaneous Raman spectroscopy (SpRS) inVia Renishaw microscope.
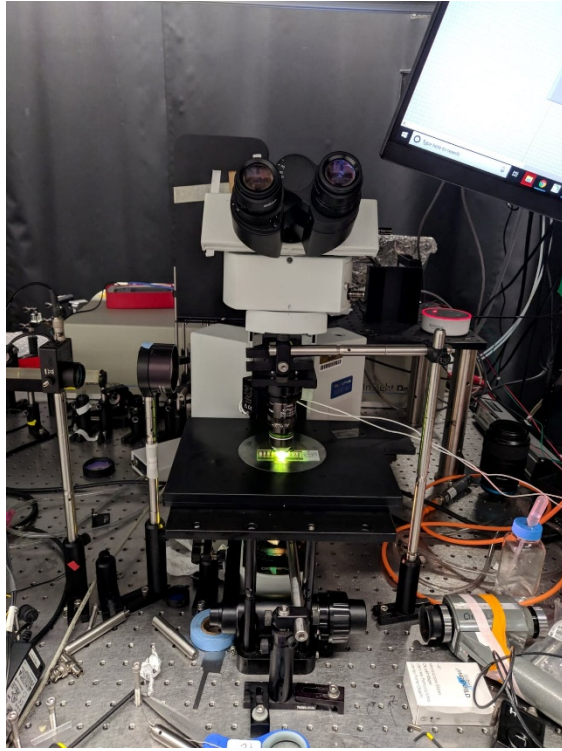
FIGURE 12.   A figure shows Stimulated Raman scattering spectroscopy (SRS).
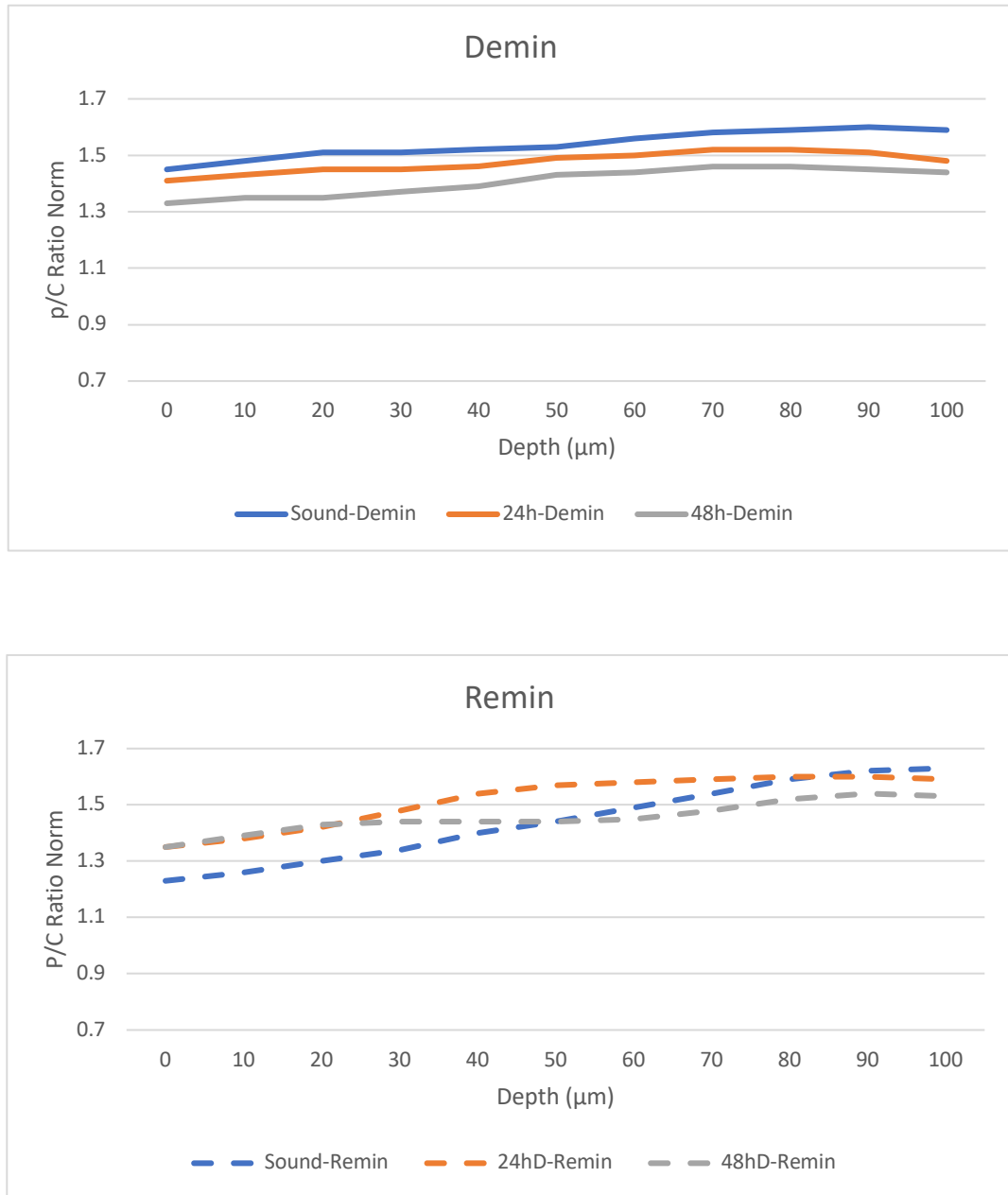
FIGURE 13. Graphs show mean of SRS P/C-Ratio for all groups of both demineralized and remineralized enamel from surface (0) to 100 μm in to dentin-enamel junction.

TABLE I

Mean and standard deviation of TMR lesion depth and integrated mineral loss (ΔZ)*

Method	Transverse Microradiography			
	Demineralization		Remineralization	
	24h	48h	24h	48h
Depth (μm)	41.5 (15.7) [1a]	64.5 (17.9) [1b]	36.1 (15.6) [1a]	55.5 (20.0) [2b]
Integrated mineral loss (ΔZ: vol% mineral×μm)	978 (322) [1a]	1621 (435) [1b]	710 (330) [2a]	1092 (463) [2b]

*Same superscript letters indicate there is not significant difference between demineralization times and same superscript numbers indicate there is not significant difference between demin and remin.

TABLE II

Mean and standard deviation of spontaneous Raman spectroscopy (SpRS) and stimulated Raman scattering spectroscopy (SRS) at surface (0 μm from the surface) for phosphate and carbonate ratio (P/C-Ratio)*

Method	P/C-Ratio					
	Demineralization			Remineralization		
	Sound	24h	48h	Sound	24h	48h
SpRS	13.0 (0.98) [1a]	12.2 (0.96) [1b]	11.9 (0.95) [1c]	13.7 (1.07) [2a]	13.6 (0.99) [2ab]	13.4 (0.89) [2b]
SRS	1.45 (0.33) [1a]	1.41 (0.42) [1b]	1.33 (0.46) [1c]	1.23 (0.48) [2a]	1.35 (0.42) [1a]	1.35 (0.42) [1a]

*Same superscript letters indicate there is no significant difference between demineralization times, and same superscript numbers indicate there is no significant difference between demin and remin.

TABLE III

Mean and standard deviation of stimulated Raman scattering spectroscopy (SRS) phosphate and carbonate ratio (P/C-Ratio) for each distance from the surface

Distance (μm)	P/C-Ratio					
	Demineralization			Remineralization		
	Sound	24h	48h	Sound	24h	48h
0	1.45 (0.33) [1a]	1.41 (0.42) [1b]	1.33 (0.46) [1c]	1.23 (0.48) [2a]	1.35 (0.42) [1a]	1.35 (0.42) [1a]
10	1.48 (0.30) [1a]	1.43 (0.38) [1b]	1.35 (0.45) [1c]	1.26 (0.49) [2a]	1.38 (0.41) [1a]	1.39 (0.41) [1a]
20	1.51 (0.27) [1a]	1.45 (0.35) [1b]	1.35 (0.44) [1c]	1.30 (0.49) [2a]	1.42 (0.39) [1a]	1.43 (0.38) [1a]
30	1.51 (0.25) [1a]	1.45 (0.30) [1a]	1.37 (0.41) [1b]	1.34 (0.49) [1a]	1.48 (0.33) [1a]	1.44 (0.35) [1a]
40	1.52 (0.22) [1a]	1.46 (0.23) [1a]	1.39 (0.40) [1b]	1.40 (0.48) [1ab]	1.54 (0.30) [1a]	1.44 (0.33) [1b]
50	1.53 (0.20) [1a]	1.49 (0.24) [1a]	1.43 (0.45) [1b]	1.44 (0.41) [1ab]	1.57 (0.29) [1a]	1.44 (0.31) [1b]
60	1.56 (0.18) [1a]	1.50 (0.21) [1a]	1.44 (0.44) [1b]	1.49 (0.35) [1ab]	1.58 (0.28) [1a]	1.45 (0.28) [1b]
70	1.58 (0.17) [1a]	1.52 (0.20) [1a]	1.46 (0.41) [1b]	1.54 (0.29) [1ab]	1.59 (0.25) [1a]	1.48 (0.27) [1b]
80	1.59 (0.18) [1a]	1.52 (0.17) [1b]	1.46 (0.38) [1c]	1.59 (0.25) [1ab]	1.60 (0.22) [2a]	1.52 (0.27) [1b]
90	1.60 (0.18) [1a]	1.51 (0.16) [1b]	1.45 (0.36) [1c]	1.62 (0.22) [1a]	1.60 (0.20) [2a]	1.54 (0.28) [1a]
100	1.59 (0.19) [1a]	1.48 (0.14) [1b]	1.44 (0.34) [1c]	1.63 (0.22) [1a]	1.59 (0.20) [2ab]	1.53 (0.32) [1b]

* Same superscript letters indicate there is no significant difference between demin times, and same superscript numbers indicate there is no significant difference between demin and remin.

TABLE IV

SpRS demineralized and remineralized enamel comparison

SRS	Sound group with p-value		24hr-D group with p-value		48hr-D group with p-value	
PC Depth 0	Demin > Remin	0.042	Demin & Remin n.s.	0.898	Demin & Remin n.s.	0.748
PC Depth 10	Demin > Remin	0.035	Demin & Remin n.s.	0.835	Demin & Remin n.s.	0.724
PC Depth 20	Demin > Remin	0.027	Demin & Remin n.s.	0.898	Demin & Remin n.s.	0.499
PC Depth 30	Demin & Remin n.s.	0.099	Demin & Remin n.s.	0.936	Demin & Remin n.s.	0.440
PC Depth 40	Demin & Remin n.s.	0.301	Demin & Remin n.s.	0.130	Demin & Remin n.s.	0.665
PC Depth 50	Demin & Remin n.s.	0.421	Demin & Remin n.s.	0.099	Demin & Remin n.s.	0.748
PC Depth 60	Demin & Remin n.s.	0.384	Demin & Remin n.s.	0.074	Demin & Remin n.s.	0.736
PC Depth 70	Demin & Remin n.s.	0.923	Demin & Remin n.s.	0.092	Demin & Remin n.s.	0.974
PC Depth 80	Demin & Remin n.s.	0.810	Demin < Remin	0.046	Demin & Remin n.s.	0.440
PC Depth 90	Demin & Remin n.s.	0.479	Demin < Remin	0.017	Demin & Remin n.s.	0.350
PC Depth 100	Demin & Remin n.s.	0.301	Demin < Remin	0.010	Demin & Remin n.s.	0.384

TABLE V

SRS inter-group comparison

SRS	Demineralization with p-value		Remineralization with p-value	
PC Depth 0	Sound > 24hr-D Sound > 48hr-D 24hr-D & 48hr-D n.s.	0.020 0.032 0.117	Sound-Remin & 24hr-D-Remin n.s. Sound-Remin & 48hr-D-Remin n.s. 24hr-D-Remin & 48hr-D-Remin n.s.	0.172 0.134 0.688
PC Depth 10	Sound > 24hr-D Sound > 48hr-D 24hr-D & 48hr-D n.s.	0.037 0.023 0.109	Sound-Remin & 24hr-D-Remin n.s. Sound-Remin & 48hr-D-Remin n.s. 24hr-D-Remin & 48hr-D-Remin n.s.	0.231 0.167 0.773
PC Depth 20	Sound > 24hr-D Sound > 48hr-D 24hr-D & 48hr-D n.s.	0.035 0.006 0.113	Sound-Remin & 24hr-D-Remin n.s. Sound-Remin & 48hr-D-Remin n.s. 24hr-D-Remin & 48hr-D-Remin n.s.	0.224 0.172 0.541
PC Depth 30	Sound & 24hr-D n.s. Sound > 48hr-D 24hr-D & 48hr-D n.s.	0.092 0.013 0.152	Sound-Remin & 24hr-D-Remin n.s. Sound-Remin & 48hr-D-Remin n.s. 24hr-D-Remin & 48hr-D-Remin n.s.	0.333 0.350 0.218
PC Depth 40	Sound & 24hr-D n.s. Sound > 48hr-D 24hr-D & 48hr-D n.s.	0.113 0.024 0.237	Sound-Remin & 24hr-D-Remin n.s. Sound-Remin & 48hr-D-Remin n.s. 24hr-D-Remin > 48hr-D-Remin	0.384 0.665 0.020
PC Depth 50	Sound & 24hr-D n.s. Sound > 48hr-D 24hr-D & 48hr-D n.s.	0.157 0.021 0.212	Sound-Remin & 24hr-D-Remin n.s. Sound-Remin & 48hr-D-Remin n.s. 24hr-D-Remin > 48hr-D-Remin	0.325 0.885 0.002
PC Depth 60	Sound & 24hr-D n.s. Sound > 48hr-D 24hr-D & 48hr-D n.s.	0.052 0.007 0.206	Sound-Remin & 24hr-D-Remin n.s. Sound-Remin & 48hr-D-Remin n.s. 24hr-D-Remin > 48hr-D-Remin	0.619 0.619 0.002
PC Depth 70	Sound & 24hr-D n.s. Sound > 48hr-D 24hr-D & 48hr-D n.s.	0.085 0.030 0.224	Sound-Remin & 24hr-D-Remin n.s. Sound-Remin & 48hr-D-Remin n.s. 24hr-D-Remin > 48hr-D-Remin	0.949 0.264 0.003
PC Depth 80	Sound > 24hr-D Sound > 48hr-D 24hr-D & 48hr-D n.s.	0.023 0.024 0.125	Sound-Remin & 24hr-D-Remin n.s. Sound-Remin & 48hr-D-Remin n.s. 24hr-D-Remin > 48hr-D-Remin	0.510 0.052 0.025
PC Depth 90	Sound > 24hr-D Sound > 48hr-D 24hr-D & 48hr-D n.s.	0.003 0.008 0.162	Sound-Remin & 24hr-D-Remin n.s. Sound-Remin & 48hr-D-Remin n.s. 24hr-D-Remin & 48hr-D-Remin n.s.	0.244 0.054 0.212
PC Depth 100	Sound > 24hr-D Sound > 48hr-D 24hr-D & 48hr-D n.s.	0.001 0.013 0.449	Sound-Remin & 24hr-D-Remin n.s. Sound-Remin > 48hr-D-Remin 24hr-D-Remin & 48hr-D-Remin n.s.	0.074 0.016 0.430

TABLE VI

Correlation between SpRS and SRS*

	SpRS P/C-Ratio		
	All	**Demin**	**Remin**
SRS P/C Ratio	0.09	0.26**	0.02

* All indicates XYZ; Demin indicates demineralization, and Remin indicates remineralization.

TABLE VII

Correlation between Transverse Microradiography (TMR)
variables and Raman spectroscopies†

Method	Transverse Microradiography					
	Depth (µm)			ΔZ (vol% mineral×µm)		
	All	Demin	Remin	All	Demin	Remin
SpRS P/C-Ratio	-0.29*	-0.39*	-0.22*	-0.38*	-0.39*	-0.31*
SRS P/C-Ratio	-0.06	-0.21*	0.11	-0.05	-0.20	0.11

†All indicates XYZ, Demin indicates demineralization and Remin indicates remineralization. *Indicates statistical significance.

TABLE VIII

Correlation between Transverse Microradiography (TMR)
mineral percent and SRS P/C-Ratio at each distance from the
enamel surface†

Distance (µm)	TMR Mineral percent (vol% mineral)		
	Demin	Remin	Change
10	0.20	-0.01	0.17
20	0.24*	-0.05	0.11
30	0.25*	-0.02	0.04
40	0.28*	0.03	-0.01
50	0.23*	0.08	0.02
60	0.21*	-0.04	-0.09
70	0.03	-0.11	-0.13
80	-0.03	-0.06	-0.11
90	-0.02	-0.03	-0.06
100	0.03	-0.03	-0.04

† Demin indicates demineralization; Remin indicates remineralization, and Change
indicates difference between Demin and Remin at each distance. *Indicates statistical
significance.

DISCUSSION

In this current study, two types of Raman spectroscopy (Spontaneous Raman spectroscopy [SpRS] and stimulated Raman scattering spectroscopy [SRS]) were used to study the artificial demineralization and remineralization process. To quantify and compare the severity of demineralization across different demineralization times (sound [0-hr], 24-hr, and 48-hr demineralization), peak ratio of phosphate and carbonate was used and calculated (P/C-Ratio). Results from the present study indicated that P/C-Ratio of both SpRS and SRS decreased as demineralization time increased with statistical significance among the treatment groups. According to a study by Robinson,[75] phosphate lost is 18.5 percent for enamel caries when compared with sound enamel, while carbonate lost is 1 percent. Thus, P/C-Ratio should be smaller in 24h-Demin and 48h-Demin based on the higher reduction of phosphate content when compared with carbonate. The enamel demineralized results from the present study support that the phosphate ratio decreased during demineralization. For inter-group comparison (sound, 24-hr, 48-hr) of remineralized specimens, P/C-Ratio of SpRS showed that remineralized groups have significantly larger P/C-Ratio than demineralized groups for all treatment groups. Artificial saliva containing phosphate was used as a remineralizing agent for our study. After remineralization, phosphate ions diffused into mineral deficient enamel, which contributes to the increasing P/C-Ratio of enamel from the demineralized baseline through the remineralization of mineral. On the other hand, carbonate content in the specimens should remain the same because carbonate was not added during the

remineralizing treatment. Results indicated that P/C-Ratio of SpRS increased after

remineralization based on the addition of phosphate content from artificial saliva.

PHOSPHATE AND CARBONATE RATIO USING
SPONTANEOUS RAMAN SPECTROSCOPY (SPRS)

After demineralization, Spontaneous Raman spectroscopy (SpRS) indicated the

phosphate and carbonate ratio was decreased, as the demineralization time increased.

According to Xu et al., P/C-ratio of sound enamel from SpRS is in the range of 12.5±

32.[11] When compared with the range of the sound enamel P/C-ratio of Xu's study, 24h-

Demin and 48h-Demin from the present study had smaller P/C-Ratio than the sound

enamel range. However, the P/C-Ratio of sound enamel from the present study showed a

range similar to Xu's study. The study from Mohanty et al. used SpRS to evaluate P/C-

Ratio of human molar enamel without any preparation in the sound and early caries

locations.[59] The results indicated P/C-Ratio for sound and early caries to be 17.14±0.15

and 14.59±1.98, respectively. The present study indicated that the average values of P/C-

Ratio for both sound and early caries are different from Mohanty's study. However, both

studies showed a similar trend, which is a larger value in the sound area and a smaller

value in dental caries. After remineralization, SpRS indicated P/C-Ratio decreased. In

addition, P/C-Ratio of remineralized groups was greater than demineralized groups in all

treatment groups with statistical significance (Sound-Remin > Sound, 24D-Remin > 24h-

Demin, 48D-Remin > 48h-Demin). This is attributed to the phosphate that was added into

the system by pH cyclic modeling, which increased the P/C-Ratio of remineralized

specimens. The increase in P/C-Ratio demonstrated that phosphate had been increased

after remineralization. Therefore, based on previous studies and the present study, SpRS

showed a pattern of P/C-Ratio for both demineralized and remineralized groups, which

could indicate the demineralization-remineralization cycle of dental caries. Based on P/C-

Ratio, SpRS could quantify remineralization and demineralization of bovine enamel.

PHOSPHATE AND CARBONATE RATIO USING
STIMULATED RAMAN SCATTERING SPECTROSCOPY (SRS)

After demineralization, stimulated Raman scattering spectroscopy (SRS)

indicated that P/C-Ratio at 0 μm decreased, as demineralization time increased. This

pattern has also been found with SpRS, The study from Ando et al. evaluated bovine

enamel artificial caries with different demineralization periods (8hr, 16hr, and 24hr).[73]

They also reported the P/C-Ratio decreased, as the demineralization time increased.

These two studies support that SRS could quantify demineralized enamel by P/C-Ratio.

After remineralization, SRS indicated that P/C-Ratio at 0 μm increased without

statistical significance. Unlike SpRS, the SRS P/C-Ratio values of remineralized groups

were smaller than demineralized groups. Phosphate was added to the system by the

remineralizing agent; thus, in theory, P/C-Ratio should have increased. There is no clear

explanation of the finding to the contrary. One of the potential explanations might be the

incorrect determination of the imaging plane from the top of the surface. To determine

the imaging plane for SRS, Raman signals are used without optically visualizing by

microscopy. Further studies are needed to confirm the ability of SRS to quantify mineral

change for remineralization. In order to improve study design, the SRS signal should be

obtained from the same location on the same specimens.

PHOSPHATE AND CARBONATE RATIO WITH DISTANCE OF
STIMULATED RAMAN SCATTERING SPECTROSCOPY (SRS)

According to Ando et al.,[73] stimulated Raman scattering spectroscopy (SRS) might be able to determine the depth of lesions from the enamel surface without specimen preparation. For the present study, after demineralization, P/C-Ratio of SRS increased from the enamel surface to 100 μm as expected. According to results from TMR in the present study, 24h-Demin and 48h-Demin lesions depth are 41.5±15.7, and 64.5±17.9 respectively. Thus, the deeper layers of 24h-Demin at 50 μm to 100 μm and 48h-Demin at 60 μm to 100 μm should be sound tooth structure. P/C-Ratio of Sound-Demin, 24h-Demin and 48h-Demin at a deeper layer (60 μm to 100 μm) should indicate similar values. However, the results of 60 μm to 100 μm indicated the highest P/C-Ratio was for Sound-Demin followed by 24h-Demin and 48h-Demin, respectively. This finding was not correlated to TMR results and was different from the results in Ando's study. According to previous studies, the enamel surface contains a high concentration of fluoride, calcium, and phosphate, which are less susceptible to acid challenge. On the other hand, the carbonate content was reported to be very minimal at the surface of enamel.[9] The greater the carbonate, the more susceptible to mineral dissolution of enamel. Thus, minimal carbonate at the outer enamel surface provides superior resistance to demineralization. The concentration of phosphate is lower moving inward to the DEJ, while the concentration of carbonate is higher.[6] For the present study, the outer surface phosphate-rich enamel was removed and polished to create a flat surface. The height of specimens was approximately 2.0 mm, and the thickness of enamel was at least 0.5 mm. The inner carbonate-rich enamel, which adjacent to DEJ, was not measured in the present

study. It obtained the SRS signal from the surface of the enamel specimen to 100 μm. Thus, the normal distribution of phosphate and carbonate content should not contribute to the unexpected P/C-Ratio outcome of 60 μm to 100 μm layers. Based on fundamental knowledge and scientific research, the explanation of this phenomenon might be found within biological variations of bovine specimens. Further studies will be needed to confirm the use of SRS to estimate lesion depth and improve the methodology.

CORRELATION

Correlation of Spontaneous Raman Spectroscopy (SpRS)
and Stimulated Raman Scattering Spectroscopy (SRS)

A correlation was found with demineralized specimens, while no correlation was found with remineralized specimens. SpRS and SRS P/C-Ratio of demineralized specimens showed the same pattern that contributes to the correlation between two methods. One the other hand, SpRS and SRS P/C-Ratio of remineralized specimens showed a different outcome because only SpRS could quantify remineralized specimens. Spontaneous Raman spectroscopy (SpRS) is based on Raman scattering by using normal far-field optics, while stimulated Raman scattering spectroscopy (SRS) is achieved through non-linear optical effects. SRS typically generates by mixing two wavelengths, spatially and temporally synchronized pulsed lasers with a pump-probe technique. The difference between the light sources of each technique may have led to a weak correlation between these methods. In addition, theoretically, the intensity of SRS should be linear to SpRS. However, the measurement of SRS can be affected by cross-phase modulation: the change in the optical phase of light beam caused by interaction with another light beam, which may cause the variations of SRS Raman spectra.

Correlation between SpRS and TMR and between SRS and TMR

For this current study, transverse microradiography was used as a reference method. Moderate correlations were found between demineralized/remineralized P/C-Ratio of SpRS and TMR (integrated mineral loss (ΔZ)/lesion depth). On the other hand, only a weak correlation between demineralized P/C-Ratio and TMR lesion depth was found for SRS. According to the results of the present study, SpRS could be able to quantify both demineralized and remineralized specimens by P/C-Ratio. For SRS, only demineralized specimens could be able to quantify by P/C-Ratio, which reflects no correlation between remineralized SRS and TMR. Ando et al. conducted a comparative study between SRS and TMR and between SRS and surface microhardness (SMH) for artificial demineralization on bovine enamel.[73] They reported the correlation between SMH-change and P/C-Ratio, and between TMR (lesion depth and ΔZ) and P/C-Ratio at some depths. Our study and Ando's study used the same method for demineralized SRS and TMR with partially different demineralized treatments (8h-16h-24h to 24h-48h). Both studies showed correlations between demineralized SRS and TMR, which indicated that SRS has the potential for mineral quantification of enamel.

Correlation between Stimulated Raman Scattering
Spectroscopy (SRS) with Depth and TMR

A weak correlation was found for 10 μm to 60 μm of demineralized specimens between SRS and TMR measurements. According to TMR, the mean of lesion depth for 24h-Demin and 48h-Demin are 41.5±15.7, and 64.5±17.9 respectively. The correlation was found at the layer that TMR showed as a demineralized area (10 μm to 60 μm). For deeper layers (70 μm to 100 μm) TMR indicated that no mineralized enamel was found

and no statistical significance differences were found among the groups. However, the

SRS P/C-Ratio between Sound, 24h-Demin, and 48h-Demin at deeper layers (70 µm to

100 µm) indicated the statistical difference between each group was not correlated to the

average lesion depth value from TMR. Thus, no correlation was found for 70 µm to 100

µm. This finding indicates that SRS might not be able to measure the depth of the lesion.

SUMMARY AND CONCLUSION

Early caries lesions were formed and characterized by Raman spectroscopy in this current study. Raman spectroscopy is a nondestructive chemical analysis method that provides information about chemical compositions, structure, and crystallinity. The combination of optical microscopy and advanced technology makes Raman spectroscopy easier to use in characterizing specimens with high resolution, which, in turn, results in better qualitative and quantitative analysis. For the present study, we conducted the direct measurement of Raman peaks of phosphate and carbonate from bovine enamel directly from the surface of specimens to quantify the demineralization and remineralization process. The ratio of phosphate and carbonate could be used to quantify demineralization and remineralization at the molecular level. Based upon our findings, we accepted the null hypothesis, because SpRS could quantify demineralization and remineralization of enamel; however, SRS could only quantify demineralization of enamel. The hypothesis was rejected for SRS enamel remineralization.

Within the limitations of this study, both spontaneous Raman spectroscopy (SpRS) and stimulated Raman scattering spectroscopy (SRS) had the potential to determine the enamel demineralization by measuring the phosphate-carbonate ratio in sound and demineralized enamel. Spontaneous Raman spectroscopy could quantify the change of remineralized enamel. The correlation was found between SpRS/SRS P/C-Ratio and integrated mineral loss (ΔZ)/lesion depth from TMR. A nondestructive caries quantification approach of spontaneous Raman spectroscopy and stimulated Raman scattering spectroscopy would benefit the early dental caries quantification.

REFERENCES

1.   Kim JK, Baker LA, Seirawan H, Crimmins EM. Prevalence of oral health problems in US adults, NHANES 1999–2004: exploring differences by age, education, and race/ethnicity. Spec Care Dent 2012;32(6):234-41.

2.   Dye BA, Thornton-Evans G, Li X, Iafolla TJ. Dental caries and sealant prevalence in children and adolescents in the United States, 2011-2012. NCHS Data Brief 2015 Mar;(191):1-8.

3.   Bagramian RA, Garcia-Godoy F, Volpe AR. The global increase in dental caries. A pending public health crisis. Am J Dent 2009;22(1):3-8.

4.   Tinanoff N, Reisine S. Update on early childhood caries since the Surgeon General's Report. Acad Pediatr 2009;9(6):396-403.

5.   Thomson W. Dental caries experience in older people over time: what can the large cohort studies tell us? Br Dent J 2004;196(2):89.

6.   Weatherell J, Robinson C, Hallsworth A. Variations in the chemical composition of human enamel. J Dent Res 1974;53(2):180-92.

7.   Ramakrishnaiah R, Rehman Gu, Basavarajappa S, et al. Applications of Raman spectroscopy in dentistry: analysis of tooth structure. Appl Spectrosc Rev 2014;50(4):332-50.

8.   Abou Neel EA, Aljabo A, Strange A, et al. Demineralization-remineralization dynamics in teeth and bone. Int J Nanomed 2016;11:4743-63.

9.   Robinson C, Weatherell J, Hallsworth A. Variation in composition of dental enamel within thin ground tooth sections. Caries Res 1971;5(1):44-57.

10.   Ko AC, Choo-Smith LP, Hewko M, et al. Ex vivo detection and characterization of early dental caries by optical coherence tomography and Raman spectroscopy. J Biomed Opt 2005;10(3):031118.

11.   Xu C, Reed R, Gorski JP, Wang Y, Walker MP. The distribution of carbonate in enamel and its correlation with structure and mechanical properties. J Mater Sci 2012;47(23):8035-43.

12.   Karlsson L. Caries detection methods based on changes in optical properties between healthy and carious tissue. Int J Dent 2010;270729.

13.   Nakornchai S, Atsawasuwan P, Kitamura E, Surarit R, Yamauchi M. Partial biochemical characterisation of collagen in carious dentin of human primary teeth. Arch Oral Biol 2004;49(4):267-73.

14. Hallsworth A, Weatherell J, Robinson C. Loss of carbonate during the first stages of enamel caries. Caries Res 1973;7(4):345-48.

15. Gao X, Elliott J, Anderson P. Scanning microradiographic study of the kinetics of subsurface demineralization in tooth sections under constant-composition and small constant-volume conditions. J Dent Res 1993;72(5):923-30.

16. Fejerskov O, Kidd E. Dental caries: the disease and its clinical management: John Wiley & Sons; 2009.

17. Featherstone JD. The caries balance: the basis for caries management by risk assessment. Oral Hlth Prev Dent 2004;2:259-64.

18. White D. The application of *in vitro* models to research on demineralization and remineralization of the teeth. Adv Dent Res 1995;9(3):175-93.

19. Ekstrand K, Zero D, Martignon S, Pitts N. Lesion activity assessment. Detection, assessment, diagnosis and monitoring of caries: Karger Publishers; 2009. p. 63-90.

20. Nyvad B, Machiulskiene V, Bælum V. Reliability of a new caries diagnostic system differentiating between active and inactive caries lesions. Caries Res 1999;33(4):252-60.

21. Ekstrand K, Bruun G, Bruun M. Plaque and gingival status as indicators for caries progression on approximal surfaces. Caries Res 1998;32(1):41-5.

22. Pretty IA, Maupomé G. A closer look at diagnosis in clinical dental practice: part 5. Emerging technologies for caries detection and diagnosis. J Can Dent Assoc 2004;70:540-41.

23. Braga MM, Ekstrand K, Martignon S, et al. Clinical performance of two visual scoring systems in detecting and assessing activity status of occlusal caries in primary teeth. Caries Res 2010;44(3):300-8.

24. Pitts N. Modern concepts of caries measurement. J Dent Res 2004;83(1_suppl):43-7.

25. Selwitz RH, Ismail AI, Pitts NB. Dental caries. Lancet 2007;369(9555):51-9.

26. Featherstone JD. Prevention and reversal of dental caries: role of low level fluoride. Community Dent Oral Epidemiol 1999;27(1):31-40.

27. Bader JD, Shugars DA, Bonito AJ. Systematic reviews of selected dental caries diagnostic and management methods. J Dent Educ 2001;65(10):960-8.

28. Lussi A. Comparison of different methods for the diagnosis of fissure caries without cavitation. Caries Res 1993;27(5):409-16.

29. Shimada Y. Caries detection in mass screening examination. Nihon Shika Ishikai Zasshi 1970;23(2):123.

30. Nyvad B, Machiulskiene V, Bælum V. Construct and predictive validity of clinical caries diagnostic criteria assessing lesion activity. J Dent Res 2003;82(2):117-22.

31. Stookey GK, Jackson RD, Zandona A, Analoui M. Dental caries diagnosis. Dent Clin North Am 1999;43(4):665-77, vi.

32. Mumford J. Pain perception threshold and adaptation of normal human teeth. Arch Oral Biol 1965;10(6):957-68.

33. Murdoch-Kinch C. Oral medicine: advances in diagnostic procedures. J Calif Dent Assoc 1999;27(10):773-80, 82-4.

34. Peers A, Hill F, Mitropoulos C, Holloway P. Validity and reproducibility of clinical examination, fibre-optic transillumination, and bite-wing radiology for the diagnosis of small approximal carious lesions: an *in vitro* study. Caries Res 1993;27(4):307-11.

35. Hintze H, Wenzel A, Danielsen B, Nyvad B. Reliability of visual examination, fibre-optic transillumination, and bite-wing radiography, and reproducibility of direct visual examination following tooth separation for the identification of cavitated carious lesions in contacting approximal surfaces. Caries Res 1998;32(3):204-09.

36. Schneiderman A, Elbaum M, Shultz T, et al. Assessment of dental caries with digital imaging fiber-optic transllumination (DIFOTITM): *in vitro* Study. Caries Res 1997;31(2):103-10.

37. Gutierrez C. DIFOTI (Digital Fiberoptic Transillumination): Validität *In vitro* [Dissertation]. LMU München: Faculty of Medicine; 2008.

38. Berg SC, Stahl JM, Lien W, Slack CM, Vandewalle KS. A clinical study comparing digital radiography and near-infrared transillumination in caries detection. J Esthet Restor Dent 2018;30(1):39-44.

39. Kühnisch J, Söchtig F, Pitchika V, et al. *In vivo* validation of near-infrared light transillumination for interproximal dentin caries detection. Clin Oral Investig 2016;20(4):821-29.

40. Abogazalah N, Ando M. Alternative methods to visual and radiographic examinations for approximal caries detection. J Oral Sci 2017;59(3):315-22.

41. Pretty I, Edgar W, Higham S. Detection of *in vitro* demineralization of primary teeth using quantitative light-induced fluorescence (QLF). Int J Paediatr Dent 2002;12(3):158-67.

42. Tranæus S, Shi XQ, Angmar-Månsson B. Caries risk assessment: methods available to clinicians for caries detection. Community Dent Oral Epidemiol 2005;33(4):265-73.

43. Lussi A, Megert B, Longbottom C, Reich E, Francescut P. Clinical performance of a laser fluorescence device for detection of occlusal caries lesions. Eur J Oral Sci 2001;109(1):14-9.

44. Gomez J. Detection and diagnosis of the early caries lesion. Paper presented at: BMC oral health, 2015.

45. Amaechi BT. Emerging technologies for diagnosis of dental caries: The road so far. J Appl Phys 2009;105(10):102047.

46. Jeon R, Han C, Mandelis A, Sanchez V, Abrams S. Diagnosis of pit and fissure caries using frequency-domain infrared photothermal radiometry and modulated laser luminescence. Caries Res 2004;38(6):497-513.

47. Jallad M, Zero D, Eckert G, Zandona AF. *In vitro* detection of occlusal caries on permanent teeth by a visual, light-induced fluorescence and photothermal radiometry and modulated luminescence methods. Caries Res 2015;49(5):523-30.

48. Diniz MB, de Almeida Rodrigues J, Lussi A. Traditional and novel caries detection methods. In: Li M (ed.) Contemporary approach to dental caries. IntechOpen; 2012.

49. Pinelli C, Serra MC, Loffredo LdCM. Validity and reproducibility of a laser fluorescence system for detecting the activity of white-spot lesions on free smooth surfaces *in vivo*. Caries Res 2002;36(1):19-24.

50. Hanlon E, Manoharan R, Koo TW, et al. Prospects for *in vivo* Raman spectroscopy. Phys Med Biol 2000;45(2):R1.

51. Kirchner M, Edwards H, Lucy D, Pollard A. Ancient and modern specimens of human teeth: a Fourier transform Raman spectroscopic study. J Raman Spectrosc 1997;28(2-3):171-8.

52. Leroy G, Penel G, Leroy N, Bres E. Human tooth enamel: a Raman polarized approach. Appl Spectrosc 2002;56(8):1030-34.

53. Rippon WB, Koenig JL, Walton AG. Laser Raman spectroscopy of biopolymers and proteins. J Agric Food Chem 1971;19(4):692-7.

54. Tsuda H, Arends J. Orientational micro-Raman spectroscopy on hydroxyapatite single crystals and human enamel crystallites. J Dent Res 1994;73(11):1703-10.

55. Tsuda H, Arends J. Raman spectroscopy in dental research: a short review of recent studies. Adv Dent Res 1997;11(4):539-47.

56. Sowa M, Mantsch H. FT-IR photoacoustic depth profiling spectroscopy of enamel. Calcif Tissue Int 1994;54(6):481-5.

57. Hill W, Petrou V. Detection of caries and composite resin restorations by near-infrared Raman spectroscopy. Appl Spectrosc 1997;51(9):1265-8.

58. Ko AC-T, Hewko M, Sowa MG, Dong CC, Cleghorn B. Detection of early dental caries using polarized Raman spectroscopy. Opt Express 2006;14(1):203-15.

59. Mohanty B, Dadlani D, Mahoney D, Mann A. Characterizing and identifying incipient carious lesions in dental enamel using micro-Raman spectroscopy. Caries Res 2013;47(1):27-33.

60. Zhan Z, Zhang X, Guo W, Xie S. Assessment of composition changes in demineralization and remineralization of human dentin using Raman spectroscopy/Beurteilung der Veränderungen in der Zusammensetzung von humanem Dentin durch Demineralisation und Remineralisation mittels Raman-Spektroskopie. Photonics Lasers Med 2013;2(1):45-50.

61. Okulus Z, Strzemiecka B, Czarnecka B, Buchwald T, Voelkel A. Surface energy of bovine dentin and enamel by means of inverse gas chromatography. Mater Sci Eng C 2015;49:382-9.

62. Huminicki A, Dong C, Cleghorn B, et al. Determining the effect of calculus, hypocalcification, and stain on using optical coherence tomography and polarized Raman spectroscopy for detecting white spot lesions. Int J Dent 2010;2010.

63. Hewko M, Sowa M. Towards early dental caries detection with OCT and polarized Raman spectroscopy. Head Neck Oncol 2010;2(S1):O43.

64. Kozloff KM, Carden A, Bergwitz C, et al. Brittle IV mouse model for osteogenesis imperfecta IV demonstrates postpubertal adaptations to improve whole bone strength. J Bone Miner Res 2004;19(4):614-22.

65. Carvalho FBd, Barbosa AFS, Zanin FAA, et al. Use of laser fluorescence in dental caries diagnosis: a fluorescence x biomolecular vibrational spectroscopic comparative study. Brazil Dent J 2013;24(1):59-63.

66. Freudiger CW, Min W, Saar BG, et al. Label-free biomedical imaging with high sensitivity by stimulated Raman scattering microscopy. Sci 2008;322(5909):1857-61.

67. Xu X, Li H, Hasan D, et al. Near-field enhanced plasmonic-magnetic bifunctional nanotubes for single cell bioanalysis. Adv Funct Mater 2013;23(35):4332-8.

68. Ji M, Orringer DA, Freudiger CW, et al. Rapid, label-free detection of brain tumors with stimulated Raman scattering microscopy. Sci Transl Med 2013;5(201):201ra119-201ra119.

69. Ozeki Y, Umemura W, Otsuka Y, et al. High-speed molecular spectral imaging of tissue with stimulated Raman scattering. Nat Photonics 2012;6(12):845.

70. Saar BG, Contreras-Rojas LR, Xie XS, Guy RH. Imaging drug delivery to skin with stimulated Raman scattering microscopy. Mol Pharm 2011;8(3):969-75.

71. Wang Z, Zheng W, Hsu C-YS, Huang Z. Polarization-resolved hyperspectral stimulated Raman scattering microscopy for label-free biomolecular imaging of the tooth. Appl Phys Lett 2016;108(3):033701.

72. Wang Z, Zheng W, Hsu SC-Y, Huang Z. Optical diagnosis and characterization of dental caries with polarization-resolved hyperspectral stimulated Raman scattering microscopy. Biomed Opt Express 2016;7(4):1284-93.

73. Ando M, Liao C-S, Eckert GJ, Cheng J-X. Imaging of demineralized enamel in intact tooth by epidetected stimulated Raman scattering microscopy. J Biomed Optics 2018;23(10):105005.

74. Irving J. Calcium and phosphorus metabolism: Elsevier; 2012.

75. Robinson C. Alterations in the composition of permanent human enamel during carious attack. Demineralisation and remineralisation of the teeth 1983:209-23.

76. Rodrigues E, Delbem ACB, Pedrini D, Oliveira M. pH-cycling model to verify the efficacy of fluoride-releasing materials in enamel demineralization. Oper Dentistry 2008;33(6):658-65.

ABSTRACT

QUANTIFICATION OF MINERALS ASSOCIATED TO ENAMEL CARIES

PROCESS BY RAMAN SPECTROSCOPY

by

Siras Sungkapreecha

Indiana University School of Dentistry
Indianapolis, Indiana

Background: Stimulated Raman spectroscopy (SRS) is a nondestructive tool for biochemical characterization of tissues. The aims were: 1) To evaluate the ability of SRS and Spontaneous Raman spectroscopy (SpRS) to differentiate among sound, demineralized and remineralized bovine enamel by phosphate and carbonate ratio (P/C-Ratio); and 2) To determine the correlation between the outcomes of transverse microradiography (TMR: Integrated mineral loss (ΔZ) and lesion depth) and P/C-Ratio.

Material and Methods: Thirty, 5×5×2-mm ground and polished bovine enamel blocks were prepared. The surface was divided into 3 equal areas. Each area was chemically demineralized (demin) by Carbopol demineralized solution for 0 (Sound-Demin), 24 (24h-Demin), and 48h (48h-Demin), respectively. Then, specimens were sectioned for TMR analysis, and the remaining one part of each specimen was

remineralized (remin) for 15days using a pH-cycling model (Sound-Remin, 24hD-Remin=24h-Demin and remineralization, 48hD-Remin = 48h-Demin and remineralization). Demin and remin groups were scanned to obtain P/C-Ratio by SpRS and SRS. SRS was further scanned from 0 (surface) up to 100 μm into the dentine at 10-μm intervals. Remineralized specimens were sectioned for TMR analysis. Wilcoxon signed-rank tests were used to compare between TMR and SpRS/SRS. Spearman correlation coefficients were used to correlate among TMR, SpRS, and SRS. A 5-percent significance level was used for each test.

Results: As demin time increased, both ΔZ and lesion depth were increased. After remineralization, both values were decreased. There were significant differences between demine and remin groups and between demin times. For SpRS, Sound-Demin had significantly larger P/C-Ratio than 24h-Demin and 48h-Demin ($p \leq 0.001$). The 24h-Demin had significantly larger values than 48h-Demin ($p = 0.048$). Sound-Remin had larger P/C-Ratio than 24hD-Remin ($p = 0.316$) and 48hD-Remin ($p = 0.015$). 24hD-Remin was larger than 48hD-Remin ($p = 0.269$). 24hD-Remin had significantly larger P/C-Ratio than 24h-Demin ($p \leq 0.001$). 48hD-Remin had significantly larger P/C-Ratio than 48h-Demin ($p \leq 0.001$). For SRS, at surface (0 μm), for demin group, Sound-Demin had significantly larger P/C-Ratio than 24h-Demin ($p = 0.020$) and 48h-Demin ($p = 0.032$). 24h-Demin had larger value than 48h-Demin; but no significant difference ($p = 0.117$). Among remin groups, Sound-Remin was not statistical significance different for 24hD-Remin ($p = 0.172$) and 48hD-Remin ($p = 0.134$). However, 24hD-Remin was smaller; but not statistical significance different from 48hD-Remin ($p = 0.688$). At deeper levels (10 μm to 100μm), it was found that 1) After demineralization, Sound-Demin had

significantly larger P/C-Ratio than 24h-Demin and 48h-Demin at 0 µm to 20 µm, and 80 µm to 100µm; Sound-Demin had significantly larger P/C-Ratio than 48h-Demin; and no statistical significance differences were found among Sound-Demin and 24h-Demin, 24h-Demin and 48h-Demin. 2) After remineralization, no statistical significance differences were found among Sound-Remin, 24hD-Remin, and 48hD-Remin. 3) Sound-Demin had significantly larger P/C-Ratio than Sound-Remin at 0 µm ,10 µm, 20 µm; and no statistical significance differences were found at levels deeper than 30 µm. 4) No statistical significance differences were found between 24h-Demin and 24hD-Remin from 0 µm to 70µm; and 24hD-Remin had significantly larger P/C-Ratio than 24h-Demin from 80 µm to 100 µm. 5) No statistical significance differences were found between 48h-Demin and 48hD-Remin. For correlation, moderate correlation was found between SpRS demineralized/remineralized groups and ΔZ, and between SpRS demineralized groups and lesion depth.

Conclusion: SpRS and SRS have the potential to quantify demineralization through calculation of the phosphate and carbonate ratio. In addition, SpRS can detect the change of remineralization. A nondestructive caries detection approach using SpRS and SRS would be beneficial in clinical practice.

CURRICULUM VITAE

Siras Sungkapreecha

September 1, 1988	Born, Bangkok, Thailand
April, 30, 2012	DDS Naresuan University Phitsanulok, Thailand
February, 2020	MSD, Cariology and Operative Dentistry Indiana University School of Dentistry Indianapolis, Indiana